RESEARCH ARTICLE

Handedness impacts the neural correlates of kinesthetic motor imagery and execution: A FMRI study

Monica Crotti[1] | Karl Koschutnig[2,3] | Selina Christin Wriessnegger[3,4]

[1]Department of Development and Regeneration, KU Leuven, Leuven, Belgium

[2]Department of Psychology, MRI Lab Graz, University of Graz, Graz, Austria

[3]BioTechMed-Graz, Graz, Austria

[4]Institute of Neural Engineering, Graz University of Technology, Graz, Austria

Correspondence

Selina Christin Wriessnegger, Institute of Neural Engineering, Graz University of Technology, Stremayrgasse 16/4, 8010 Graz, Austria.
Email: wriessnegger@tugraz.at

Abstract

The human brain functional lateralization has been widely studied over the past decades, and neuroimaging studies have shown how activation of motor areas during hand movement execution (ME) is different according to hand dominance. Nevertheless, there is no research directly investigating the effects of the participant's handedness in a motor imagery (MI) and ME task in both right and left-handed individuals at the cortical and subcortical level. Twenty-six right-handed and 25 left-handed participants were studied using functional magnetic resonance imaging during the imagination and execution of repetitive self-paced movements of squeezing a ball with their dominant, non-dominant, and both hands. Results revealed significant statistical difference ($p < 0.05$) between groups during both the execution and the imagery task with the dominant, non-dominant, and both hands both at cortical and subcortical level. During ME, left-handers recruited a spread bilateral network, while in right-handers, activity was more lateralized. At the critical level, MI between-group analysis revealed a similar pattern in right and left-handers showing a bilateral activation for the dominant hand. Differentially at the subcortical level, during MI, only right-handers showed the involvement of the posterior cerebellum. No significant activity was found for left-handers. Overall, we showed a partial spatial overlap of neural correlates of MI and ME in motor, premotor, sensory cortices, and cerebellum. Our results highlight differences in the functional organization of motor areas in right and left-handed people, supporting the hypothesis that MI is influenced by the way people habitually perform motor actions.

KEYWORDS
cerebellum, fMRI, handedness, motor execution, motor imagery, RRID:SCR_002502, RRID:SCR_016216

Highlights

- We are the first to investigate brain activity during different motor imagery (MI) and motor execution (ME) tasks in both left- and right-handed participants.
- We found significant differences ($p < 0.05$) in brain activity between left- and right-handed participants during both MI and ME.
- During MI in both groups, the highest peak was found over the ipsilateral hemisphere for MI task.
- During MI, only right-handers showed the involvement of the posterior cerebellum.
- MI is influenced by the way people habitually perform motor actions.

Significance

The present research investigates whether right and left-handers show differences in terms of brain activity (i.e., area involved) when they perform or imagine a movement with the right, left, or both hands. The study was performed with functional magnetic resonance imaging and for the first time the same paradigm was applied to both right and left-handers. Our results show significant differences in brain activity between the groups during both motor imagery and movement execution. Such results could be used to exploit new clinical assessments as well to ameliorate rehabilitation planning (e.g., personalized treatment).

1 | INTRODUCTION

Nine out of 10 individuals in the world (Baraldi et al., 1999; Kim et al., 1993; Singh et al., 1998) show right-hand dominance. Although handedness is the primary manifestation of hemispheric lateralization, it is still debatable how this preference is reflected in the motor organization of the brain. Studies over the past decades have found agreement on the activation of the primary motor and sensory areas, as well as the motor association areas and cerebellum for complex movement production. Additionally, several functional magnetic resonance imaging (fMRI) studies revealed contralateral and ipsilateral activation within motor-related areas (Baraldi et al., 1999; Kim et al., 1993; Singh et al., 1998). Although the main observed activity for unimanual movement is on the contralateral primary motor cortex (M1) and ipsilateral cerebellum, activations have also been detected on the same side of the performing hand. In the study of Kim et al. (1993), results showed that the right motor cortex was activated during contralateral movements in both right and left-handers. Left motor cortex activity was instead found during ipsilateral movements in both groups and seemed more pronounced in right-handed participants. Nevertheless, there is also evidence of no difference in brain activation in left and right-handers (Dassonville et al., 1997) and results supporting that only left-handers have bilateral activation in the lateral premotor cortex (Kawashima et al., 1997). A further question of interest is whether these differences are present during motor imagery (MI) tasks.

MI is defined as an internal representation of simple or complex movements in the absence of physical action, meaning that it is not accompanied by any kind of peripheral muscular activity (Annett, 1995; Jeannerod, 1995; Porro et al., 1996). Jeannerod (1995) first differentiated it from the broader class of mental imagery, a quasi-perceptual experience occurring in the absence of perceptual input (Cattaneo & Silvanto, 2015). According to the author, MI is part of motor representation, a broader phenomenon related to planning and preparing movements. More precisely, if motor representation usually is a nonconscious process, MI represents conscious access

to the content of a movement. Thus, MI and motor representation would share functional properties (i.e., motor images), suggesting a functional equivalence in the causal role of movement generation. Several neuroimaging studies attempted to disentangle this question finding mixed results (Decety, 1996; Fitts & Peterson, 1964; Jeannerod, 1994, 1995; Viviani & Schneider, 1991). Overlapping activations were found in primary motor cortex (M1), supplementary motor area (SMA), premotor cortex (PMC), inferior parietal lobule (IPL), superior parietal lobule (SPL), primary somatosensory (S1) cortex, and cerebellum (Gerardin, 2000; Guillot et al., 2008; Hanakawa et al., 2003; Lotze et al., 1999; Michelon et al., 2006; Roth et al., 1996; Solodkin et al., 2004; Szameitat et al., 2007a). Concerning subcortical areas, ipsilateral cerebellar activity over lobules V and VIII (van der Zwaag et al., 2013) has been reported for movement execution (ME) of unimanual tasks with lobules IV, V, and VIII considered representing the cerebellar homunculus (Mottolese et al., 2013). While anterior cerebellar lobules project to contralateral cerebral cortical motor-related areas, the cerebellar hemispheres are mainly connected to contralateral cerebral association networks (Bostan et al., 2013; Buckner, 2013; Buckner et al., 2011). Thus, if anterior lobules (lobules I–V) are associated with the execution of ipsilateral simple, repetitive movements, functional heterogeneity was reported for the superior-posterior cerebellum. In detail, higher-order cognition is associated with Crus I and Crus II and a combination of complex motor and cognitive functions is linked to lobules VI and VIIb. Furthermore, there is evidence that the posterior cerebellum (lobules VI through IX) is involved in the inhibition of ME (Lotze et al., 1999) and lobule VI in cognitively demanding tasks (Stoodley et al., 2012) and MI (Sakai et al., 1999; for a Review see Hétu et al., 2013). Although further evidence suggests that MI and ME networks are distinct (Gao et al., 2011; Gerardin, 2000; Jeannerod, 2001; Stephan & Frackowiak, 1996; Vigneswaran et al., 2013), it is generally accepted that the distribution of activation tends to be similar.

What it is still lacking is understanding how MI differs across individuals on the base of their experience both at the cortical and subcortical levels.

With specific regard to hand movements and handedness, the question is whether MI neural correlates vary between right and left-handers and to which extent this difference is resembling the one found for ME. In this view, MI should be considered "body-specific" (Casasanto, 2009), meaning that it is influenced by how people habitually perform motor actions. Casasanto (2009) found that during MI for complex hand actions, the activation of cortical areas involved in motor planning and execution was left-lateralized in right-handers but right-lateralized in left-handers. Thus, MI reflects the difference found for ME between right and left-hander, supporting that long-term motor history (i.e., a preference to execute an action with one hand) also influences MI. This is in line with the "simulation hypothesis" (Decety, 1996; Jeannerod, 1994, 1995), where MI of action involves the recruitment of the same neural networks in the motor system that are engaged when the movement is actually being executed. An alternative position defines MI as a more abstract implementation of general kinematic rules of biological motion, such as the selection of an action's goal (Fitts & Peterson, 1964; Viviani & Schneider, 1991). Hence, the motor plan generated during MI is abstracted away from the individual motor experience or specific effectors and occurs at the level of goal of the imagined action (Rijntjes et al., 1999). Rijntjes et al. (1999) showed that movement parameters of highly trained movement are stored in secondary sensorimotor cortices of the extremity with which it is usually performed (i.e., dorsal and ventral lateral premotor cortices). These areas are, therefore, functionally independent from the primary representation of the effector. This issue is still in debate and several approaches have been used to address this question (e.g., EEG, fMRI, brain-damaged patients, behavioral techniques), finding mixed results in support of one of the two hypotheses.

Overall, most research supports the "simulation hypothesis" (Decety, 1996; Jeannerod, 1994, 1995) reporting EEG and fMRI studies which were able to discriminate MI tasks according to the specific effector imagined. For instance, the results of the study of Perruchoud et al. (2016) illustrate how our brain is specialized in representing visual and sensorimotor aspects of our body. More in detail, they highlighted the difference between hand and body MI in recruiting two distinct brain networks (i.e., local and global bodily representations).

Furthermore, different fMRI studies suggest that hand posture influences MI (Nico, 2004; Shenton et al., 2004). Ehrsson et al. (2003) showed that MI of hand movements activates the hand sections of the contralateral motor-related areas (i.e., M1, dPM, PCC, and SMA). Consistent with this hypothesis, Szameitat et al. (2007) demonstrated that during MI of complex everyday movements different lateralization in right-handers was found when imagining actions with the right hand as compared to actions with the left hand. Willems et al. (2009) demonstrated differential and opposite lateralization for the two groups during MI of action verbs, suggesting that right- and left-handers represent action verb meanings from an egocentric perspective, which reflects the way they perform these actions with their dominant hand. Additional findings from Gentilucci et al. (1998) postulated differences in the MI mechanism between

left and right-handers, suggesting that the former rely more on a pictorial hand representation, whereas the latter on a pragmatic one.

Thus, fMRI studies corroborate the hypothesis that right and left-handed individuals show different sensorimotor processing reflected in distinct brain activity patterns during MI tasks. With specific regard to handedness, it implies that activation of motor areas during MI is different in right- and left-handed individuals.

Although these differences have been highly investigated, the majority of fMRI studies concern only right-handed participants. Furthermore, to the best of our knowledge, there is no study directly investigating the difference between right and left-handers' MI neural correlates per se and especially in the cerebellum. To achieve a deeper understanding of handedness effects on MI in both right and left-handed individuals, the present study used fMRI to compare neural correlates associated with the execution and imagination of a simple task (i.e., squeezing a ball) with the dominant, non-dominant, and both hands.

2 | MATERIALS AND METHODS

2.1 | Participants

Fifty-one healthy participants, 26 right-handed (13 males and 13 females) and 25 left-handed (12 males and 13 females), between 19 and 32 years of age (mean = 24.61 years; SD = 3.09) volunteered to participate in the experiment for compensation of 20 euros (Table 1). Exclusion criteria included any major medical illness that could impact brain function, such as neurological or psychiatric conditions. Besides, no participants had any contraindications to MRI such as having chronic diseases, being under medication, being pregnant, having metallic or electrically conductive implants or prostheses, having tattoos on the head or neck area, nicotine patches, or cosmetic eye manipulations. All participants were informed about the purpose of the study before giving their written consent. The study was approved by the local ethics committee (Medical University of Graz) and is in accordance with the ethical standards of the Declaration of Helsinki. Handedness assessment was calculated for each participant through the Edinburgh Handedness Inventory (EHI; Oldfield, 1971) and Hand Dominance Test (HDT; Steingrüber & Lienert, 1971). At the end

TABLE 1 Demographic characteristics of the sample (N = 51)

Number	51
Age	M = 24.61 (SD = 3.09)
Handedness	
Right = 26	Male = 13
	Female = 13
Left = 25	Male = 12
	Female = 13

Note: Data are presented as sample size (N) for number and handedness. Right = right-handed; Left = left-handed. Age is reported in terms of mean (M) and standard deviation (SD).

of the experiment, they were also asked to fill the second version of the Vividness of Movement Imagery Questionnaire (VMIQ-2; Kinesthetic part only; see Extended Data Figure 6) to assess participants' kinesthetic MI ability.

2.2 | Anti-COVID-19 measures

This study took place in accordance with the recommended measures of the Austrian Ministry of Social Affairs. All employees in the laboratory wore mouth and nose protection (MNS) and maintained a distance of 1 m from each other. The maximum number of study participants present in the laboratory was one person at any time and all employees checked their state of health daily using a COVID-19 questionnaire (see Extended Data Figure 7). To clarify whether there was a suspected corona case, we request the COVID-19 questionnaire to each participant who was allowed to enter the laboratory only if such a questionnaire was available and checked. Participants were picked up at a meeting point outside the university building. This was followed by the review of the questionnaire as well as the participant side setting up of MNS. Participants were always accompanied when entering and leaving the laboratory, and participants were not allowed to meet at any time. Participants wore MNS when they entered the laboratory and were asked to wash their hands. The person authorized to carry out the MR measurement wore MNS (FFP2) and a face shield. Participants kept their MNS on until immediately before attaching the head coil and then removed it themselves (at the end of the measurement, it was put back on before leaving the scanner room). After the measurement, all objects that were in direct contact or in close proximity to the test participants were disinfected (Incidin TM Liquid; required minimum exposure time 10 min sufficient for the surface disinfection). The scanner room has an exhaust system. All other rooms were ventilated for 5 min. The next participant was allowed to enter the laboratory only when the cleaning and disinfection were completed.

2.3 | Procedure

Each session lasted around one and a half hours and took place in two separate rooms at the MRI Lab Graz. The whole experiment included two phases: the preparation phase and the fMRI scanning. The first part (i.e., preparation phase) took place in a separate room equipped with a computer, a table, and chairs. Here, the participants were asked to read an information letter in which they were given further information about the study, fill and sign the informed consent and the participant protocol.

In order to assess hand dominance, each participant completed the Hand Dominance Test (HDT; Steingrüber & Lienert, 1971). Then, to familiarize themselves with the experimental conditions, all participants were instructed to squeeze a ball several times at their own pace. Next, the concept of MI was explained verbally and through a written definition which provides the precise difference between kinesthetic, internal, and external visual imagery. Then, they were instructed to "imagine repeatedly squeezing the ball with kinesthetic perspective at your own pace during the task periods of 'Imagery' and not to change the pace during the experiment." Once they felt ready, a short version of the paradigm was shown, including both the execution and imagery tasks presented on the computer.

The second phase started with the preparation according to the safety measurements for undergoing an MRI session. Then, the participant entered the scanner room where he performed in a single session both the imagery and execution tasks. Participants were lying on the scanner table and cushions were used to reduce head motion. Earplugs were also provided to reduce MRI scanner noise. Verbal instructions were repeated through a microphone from the outside of the scanner room, and once the participant felt ready, scanning started.

The first block included 3.47 min of T1 structural MRI (Figure 1). The second block was the MI task. Both conditions (i.e., MI and ME) had the same visual input. To create the stimulus material, we took photographs of a model naturally squeezing a ball using the right hand, left hand, and both hands (Figure 1). Visual stimuli were presented on an LCD screen (NNL MR compatible 32-inch monitor) with Presentation Version 20.0 Build 07.26.17 (Neurobehavioral System, Inc., www.neurobs.com). Participants looked at the screen located at the backside of the scanner through a mirror system. Each participant performed first the imagination task and then the execution task. We decided not to randomize the order of the tasks (i.e., MI, ME) since previous studies showed that just a few minutes of motor exercise on the eve of the imagery task leads to stronger cerebral activation in motor-related areas (Wriessnegger et al., 2014). Thus, to prevent ME influence on the cerebral activation, each participant performed the two tasks in the following order: (1) "Imagery," where participants imagined squeezing a foam ball (7 cm diameter) with the right, left, or both hands without holding the ball; (2) "Execution," where participants squeezed the foam ball (7 cm diameter) with the right, left, or both hands while holding the ball. Only at the beginning of the MI task, the word "Imagery" appeared on the screen. Each trial started with a fixation cross, followed by a picture showing a right hand, left hand, or both hands indicating which condition had to be executed. The order of trials for each condition (left/right/both hands) was randomized across participants. Thirty trials of 7 s for each condition (left/right/both hands) were randomized across participants. A jitter interval between 5 and 9 s of resting time (fixation cross) took place between trials. Thus, the duration of the task was not the same for all the participants. The MI task lasted for approximately 20 min. Then, participants could rest for 5 min while DTI data were acquired. ME task followed. Before the ME run started, the experimenter entered the scanner room to provide the balls to the participant. Only at the beginning of the ME task, the word "Execution" appeared on the screen. ME task included 30 trials of 7 s for each condition (left/right/both hands) randomized across participants. A jitter interval between 5 and 9 s of resting time took place between trials. Thus, the duration of the task was not the same for all the participants. The ME task lasted for approximately 10 min. After the experiment, the participants filled out the modified version of the VMIQ-2 concerning the kinesthetic modality only.
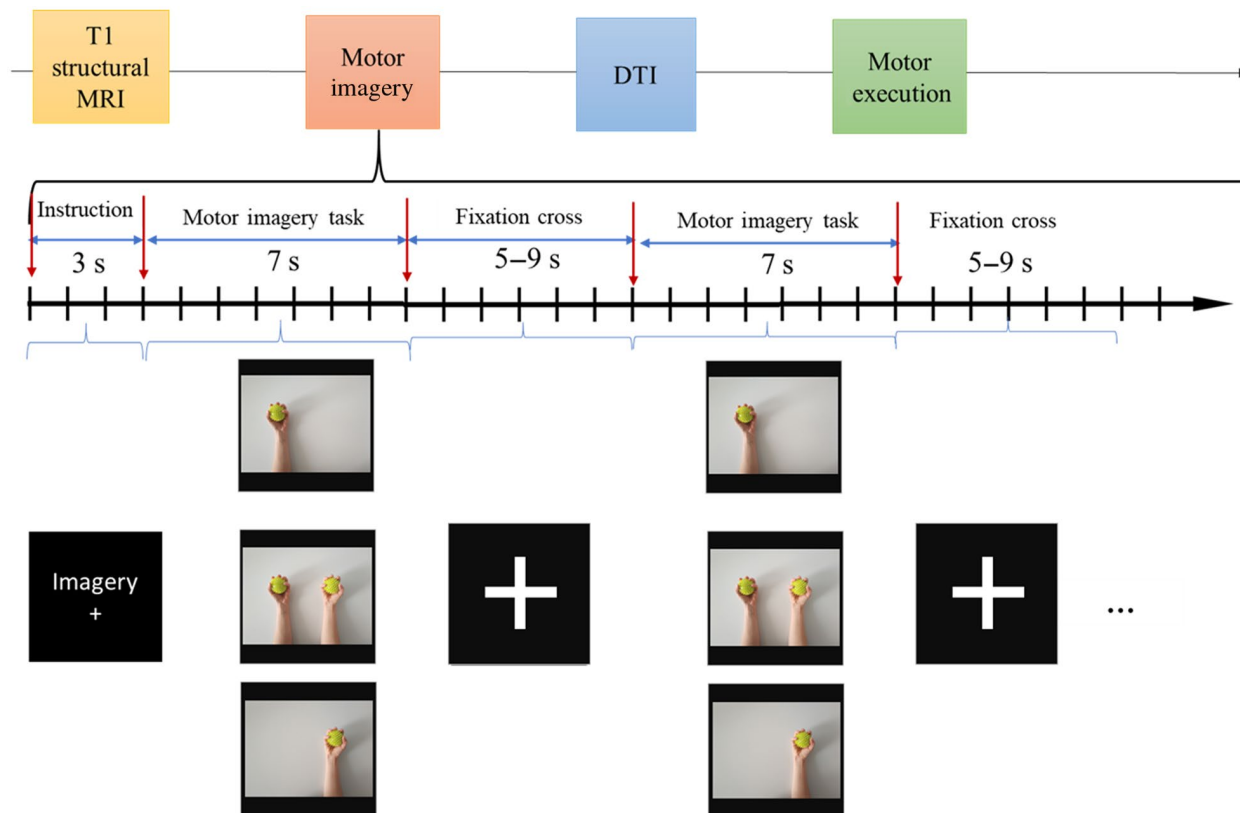
FIGURE 1 Timeline of the experiment. The trial started with 3.47 min of T1 structural MRI followed by the motor imagery (MI) task (approximately 20 min). DTI data were then acquired (5 min), followed by the motor execution (ME) task (approximately 10 min). Detailed timing of the motor imagery task is here displayed. Only at the beginning of the MI task, the word "Imagery" appeared on the screen. Each trial started with a fixation cross (3 s) followed by a picture showing a right hand, left hand, or both hands indicating which condition had to be executed (7 s). A jitter interval between 5 and 9 s of resting time (fixation cross) took place between trials. Trials for each condition (left/right/both hands) were randomized across participants. The same procedure was applied for the ME task with the only difference that at the beginning the word "Execution" was displayed

2.4 | Paradigm validation

To control for active movements during the MI task, participants were observed through a monitor while no electromyogram (EMG) was recorded over participants' hands. To validate the MI task, we performed a multivariate pattern analysis with ProNTo v.2.1 (Schrouff et al., 2013). A support vector machine (SVM) classification was performed to find differences between whole-brain functional maps of left and right MI. We used the "Leave One Subject per Group Out" Cross-Validation scheme. Results indicate a very good classification for the two different imagery tasks (See Figure 8 in the Extended Data). With a total accuracy of 93.62% and a balanced accuracy for left MI of 91.49 and 95.74% for right MI, we can be quite certain that all participants were engaged in the task.

2.5 | Image acquisition

The experiment was conducted using a 3T MRI scanner (SIEMENS Magnetom VIDA, Syngo MR XA20) at the MRI Lab Graz. A 64-channel head coil was used for acquisition. High-resolution T1-weighted anatomical 3D scans were recorded and reconstructed in sagittal plane (MPRAGE sequence; voxel size $1.0 \times 1.0 \times 1.0$ mm^3, number of slices = 192, repetition time (TR) = 1,600 ms, echo time (TE) = 2.36 ms, flip angle = 9°). Functional images were acquired using SIEMENS SMS EPI (Simultaneous Multislice Echoplanar Imaging) sequence with the following parameters: voxel size = $1.8 \times 1.8 \times 1.8$ mm^3, number of slices = 78, TR = 2,300 ms, TE = 30.00 ms, flip angle = 72° SMS factor = 3, parallel imaging with acceleration factor = 2 (total PAT = 6) using an interleaved multi-slice mode for each experimental session (i.e., Imagery and Execution). Functional images were acquired using AP phase encoding direction. Field maps were acquired with inverse coding direction. Multishell DTI images were acquired using SIEMENS SMS EPI (Simultaneous Multislice Ecoplanar Imaging) sequence with voxel size = $2.5 \times 2.5 \times 2.5$ mm^3, number of slices = 57, TR = 2,800 ms, TE = 95.00 ms, SMS factor = 3, parallel imaging with acceleration factor = 2 (total PAT = 6) using fat-saturation. A custom diffusion vector set with 100 directions and the following b-values ($b = 0$; 1,000; 3,000 s/mm^2) was used.

2.6 | Data analysis

The software packages used for preprocessing was fMRIPrep 20.1.1 (Esteban, Blair, et al., 2018; Esteban, Markiewicz, et al., 2018; RRID:SCR_016216), which is based on Nipype 1.5.0 (Esteban, Markiewicz, et al., 2018; Gorgolewski et al., 2011; RRID:SCR_002502).

fMRI first-level data analysis was performed using Fitlins (version: 0.6.2, 2017–2019, Center for Reproducible Neuroscience; https://github.com/poldracklab /fitlins). For each participant, a random-effects analysis (RFX) of the activation during each of the three experimental conditions (i.e., right-hand, left-hand, and both hand execution) was performed for the two runs (i.e., MI and ME). To test for condition effects at the first level, a general linear model was constructed with the following regressors of interest: left, right, and both hands. Additionally, we also modeled regressors of no interest, such as framewise displacement, three axial translation, three axial rotation, five a_comp_cor, and eight drifts. The contrasts of interest were the experimental condition effects (left > right; both > right; both > left; both > fixation; left > fixation; and right > fixation) for a total number of six contrasts for both the execution and imagery runs. The activation–fixation contrast images based on the SPM model were then taken to a second-level random-effects analysis to test for group effects.

GLM Flex Fast2 (Schultz, 2017) based on MATLAB2019a (Mathworks, Inc., Natick, MA) was used for the second-level analysis. This tool has the advantage of using a common notation and can handle between- and within-participant designs. The contrasts from Fitlins were entered into a random-effects group analysis. A *t* test was performed for each contrast with $p < 0.05$. Our model was defined as follows:

$$Group * Hand * Condition + random(SS|Hand * Condition)$$

Due to problems with the Fitlins model estimation, we had to exclude two participants for the ME and four participants for the MI task. The final sample included 45 participants, 25 right-handed and 20 left-handed (Table 2). Post hoc contrasts were specified in GLM FlexFast2 for both the between and within-group analysis. A 2×3 within-participant design (*t* test, $n = 45$; $p < 0.05$) was specified to investigate if there was any difference for the two tasks (i.e., MI and ME) and two conditions (i.e., left and right) for a total number

of four contrasts per group (i.e., MEleft>MEright; MIleft>MIright; MEleft>MIleft; and MEright>MIright).

A 2×3 between-participant design (*t* test, $n = 45$; $p < 0.05$) was specified to investigate any difference between the left and right groups for the two tasks (i.e., MI and ME) and three conditions (i.e., left, right, and both hands). All the contrasts were then thresholded with a FWE voxel correction ($p < 0.05$) with bspm-view (Spunt, 2016) based on SPM8/SPM12 operating in MATLAB 2019b.

3 | RESULTS

3.1 | Behavioral results

3.1.1 | Edinburgh handedness inventory (EHI)

On the Edinburgh Handedness Inventory (EHI), participants' results were the following: mean = 11.08, *SD* = 75.69, range −100 to −100. Twenty-six participants were right-handed (N = 26, 12 female, mean age 24.23, range 21–32 years, EHI score: mean = 76.92, *SD* = 14.49, range 50–100), three were mixed-handed (N = 3, 1 female, mean age 22.67, range 21–24 years, EHI score: mean = 11.67, *SD* = 32.53, range −20 to 45), and 22 were left-handed (N = 22, 12 female, mean age 25.32, range 19–30 years, EHI score: mean = −66.82, *SD* = 39.56, range −100 to 90).

3.1.2 | Hand dominance test (HDT)

On the Hand Dominance Test (HDT), participants' results were the following: mean = 101, *SD* = 75.69, range 93 to 108. Twenty-five

TABLE 2 Demographics characteristics of the final sample (N = 45)

Number	45	
Handedness		
Right = 25	Male = 12	
	Female = 13	
Left = 20	Male = 11	
	Female = 9	

Note: Data are presented as sample size (N) for number and handedness. Right = right-handed; Left = left-handed.
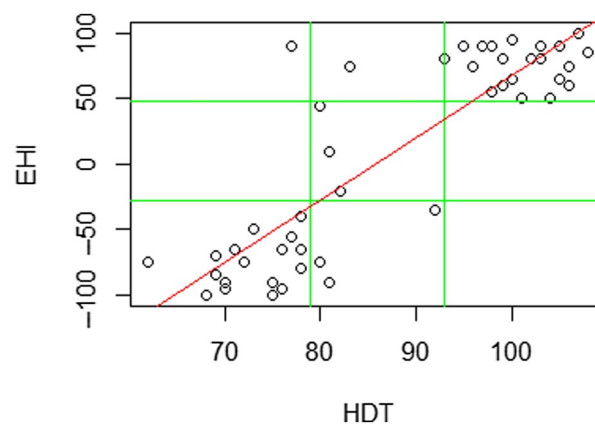

FIGURE 2 Correlation plot between the Edinburgh Handedness Inventory (EHI) and the Hand Dominance Test (HDT). The score for each participant for the EHI are displayed on the *y* axis and those for the HDT on the *x* axis. Higher scores indicate right-handed participants for both the EHI and the HDT. Green lines define the cutoff scores for groups; the red line displays the regression line between the two test scores. A significant correlation ($r = 0.866$) was found between EHI and the HDT scores
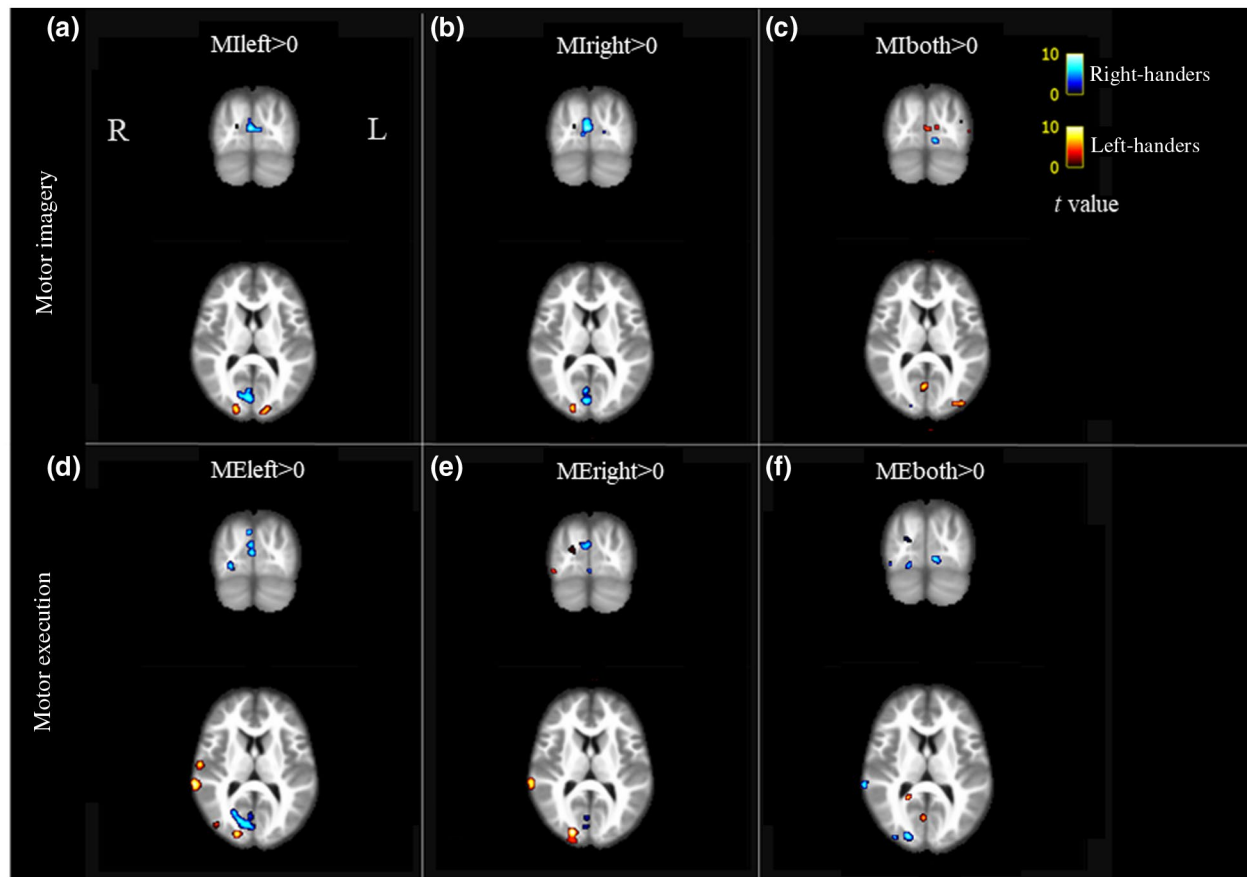
FIGURE 3 Between-group contrasts for motor imagery and motor execution (ME). (a–c) Between-group contrasts (*t* test, *n* = 45; *p* < 0.05) for motor imagery (MI). (d–f) Between-group contrasts (*t* test, *n* = 45; *p* < 0.05) for ME. Contrasts are shown for left hand (a,d), right hand (b,e), and both hand (c,f) conditions in comparison with "fixation" (0). Suprathreshold (FWE voxel *p* < 0.05) voxels for right-handers are shown in blue and in red for left-handers. Position MNI coordinates [12 −86 12]; right hemisphere (R) is displayed on the left side, left hemisphere (L) on the right side

participants were right-handed (*N* = 25, 11 female, mean age 24.36, range 21–32 years, HDT score: mean = 101, *SD* = 7.3, range 93–108), seven were mixed-handed (*N* = 7, 3 female, mean age 25, range 21–30 years, HDT score: mean = 82.29, *SD* = 4.57, range 78–92), and 19 were left-handed (*N* = 19, 11 female, mean age 24.79, range 19–30 years, HDT score: mean = 73.32, *SD* = 4.59, range 62–81).

3.1.3 | Correlation analysis

A Pearson correlation analysis was run between the EHI and the HDT for assessing if self-report measurements were correlated with the results of participants' performances. A significant correlation (*r* = 0.866) was found between EHI and the HDT scores (Figure 2). Furthermore, given the nature of the data for the EHI and HDT, a Cohen's kappa analysis was performed. According to the result (wk = 0.3271640), we can state that our tests, EHI and EDT, have a fair agreement.

Our final sample was divided into two groups, namely right and left-handed. Since the correlation between the two tests was high, we decided to divide our groups according to the result of the self-report EHI. Hence, three participants were scored as mixed handers and when asked "Do you consider yourself right or left-handed?," they all replied "left-handed." For this reason, we decided to include them in the left-handed group.

3.1.4 | VMIQ-2

On the VMIQ-2, participants' results were the following: mean = 24.25, *SD* = 6.87, range 13 to 40, mode = 29. The lower the score, the more vivid is the imagination. Being the test formed by 12 items with a rating score between 1 and 5, the minimum score achievable is 12 and the maximum is 60. Despite the subjectivity of this measurement, we think that the VMIQ-2 can be considered as a good self-report index about participants' imagery ability.
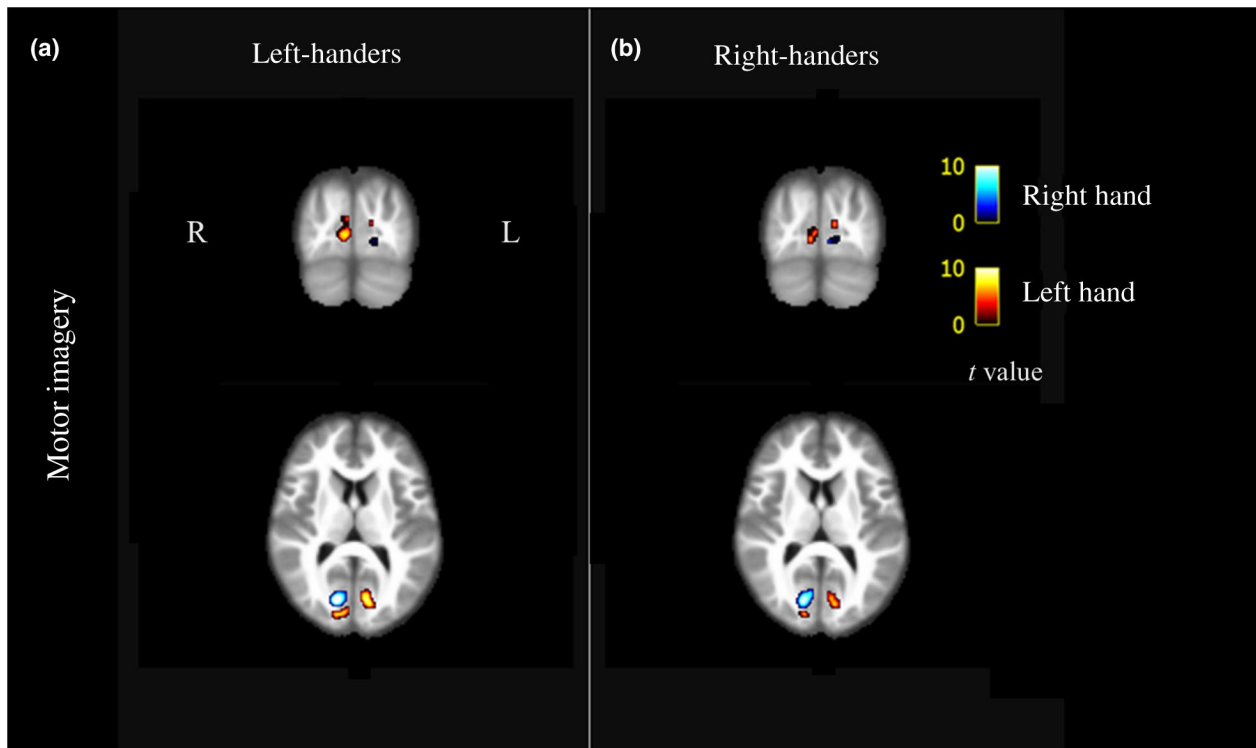
FIGURE 4 Within-group contrasts for motor imagery. Within-group contrasts (*t* test, *n* = 45; *p* < 0.05) for motor imagery (MI) for the left-handed group (a) and right-handed group (b). Suprathreshold (FWE voxel *p* < 0.05) voxels for right-hand MI in comparison with "fixation" are shown in blue and for left-hand MI in comparison with "fixation" in red. Position MNI coordinates [12 −86 12]; right hemisphere (R) is displayed on the left side and left hemisphere (L) on the right side

3.2 | fMRI

All participants performed the task sequences correctly at their own pace. No overt movement was observed during the imagery tasks. A complete overview of the results from the GLM-Flex analysis for both main effects and interactions is displayed in Table 3 in the Extended Data.

Voxel-wise FWE-corrected threshold images were computed with "bspmview" and for each contrast, we obtained a table showing all local maxima separated by more than 20 mm. Regions were automatically labeled using the Anatomy Toolbox atlas (Eickhoff et al., 2005) (see Tables 4–6 in the Extended Data).

Contrast images were then displayed on mrview based on MRtrix3 (Tournier et al., 2019). We first describe the between-group results comparing MI and ME for right, left, and both hands (i.e., MIleft>0; MIright>0; MIboth>0; MEleft>0; MEright>0; and MEboth>0). In the described contrasts, zero is the fixation cross. Within-group results are then displayed, comparing right and left-hand tasks for right and left-handers separately (i.e., MEleft>MEright and MIleft>MIright). Then, to make a direct comparison of the two tasks (i.e., MI and ME) in both the groups, we discuss the contrasts between ME and MI of the same hand (i.e., MEleft>MIleft and MEright>MIright) with a specific focus of the cerebellum.

3.2.1 | Between group

To verify the hypothesis of whether there was any significant difference between the left and right-handed group, a two-sample *t* test (*p* < 0.05, FWE corrected for voxel) for all the contrast of interest was run.

Among MI conditions, significant group effects (*p* < 0.05) were found for the following contrasts, namely MIleft>0 (Figure 3a), MIright>0 (Figure 3b), and MIboth>0 (Figure 3c). Here again, zero is the fixation cross.

For the left MI task, the right-handed group showed a predominantly left-lateralized activation pattern (Figure 3a, blue) compared to the left-handed group. The activation included the left lingual gyrus and left cerebellum (Crus 1) and a small cluster on the right inferior temporal gyrus. In the left-handed group, left MI yielded a more bilateral activation pattern (Figure 3a, red), including the right calcarine gyrus and the left posterior-medial frontal and left superior occipital gyrus.

In the right-handed group, "right MI" comparison with "fixation" induced a bilateral activation pattern (Figure 3b, blue), including the right calcarine gyrus, left lingual gyrus, and fusiform gyrus, while the left-handed group (Figure 3b, red) showed a right-lateralized activation pattern over the calcarine gyrus. The direct comparison of these two contrasts revealed a similar pattern for the two groups, showing a bilateral activation for MI of the dominant hand and a
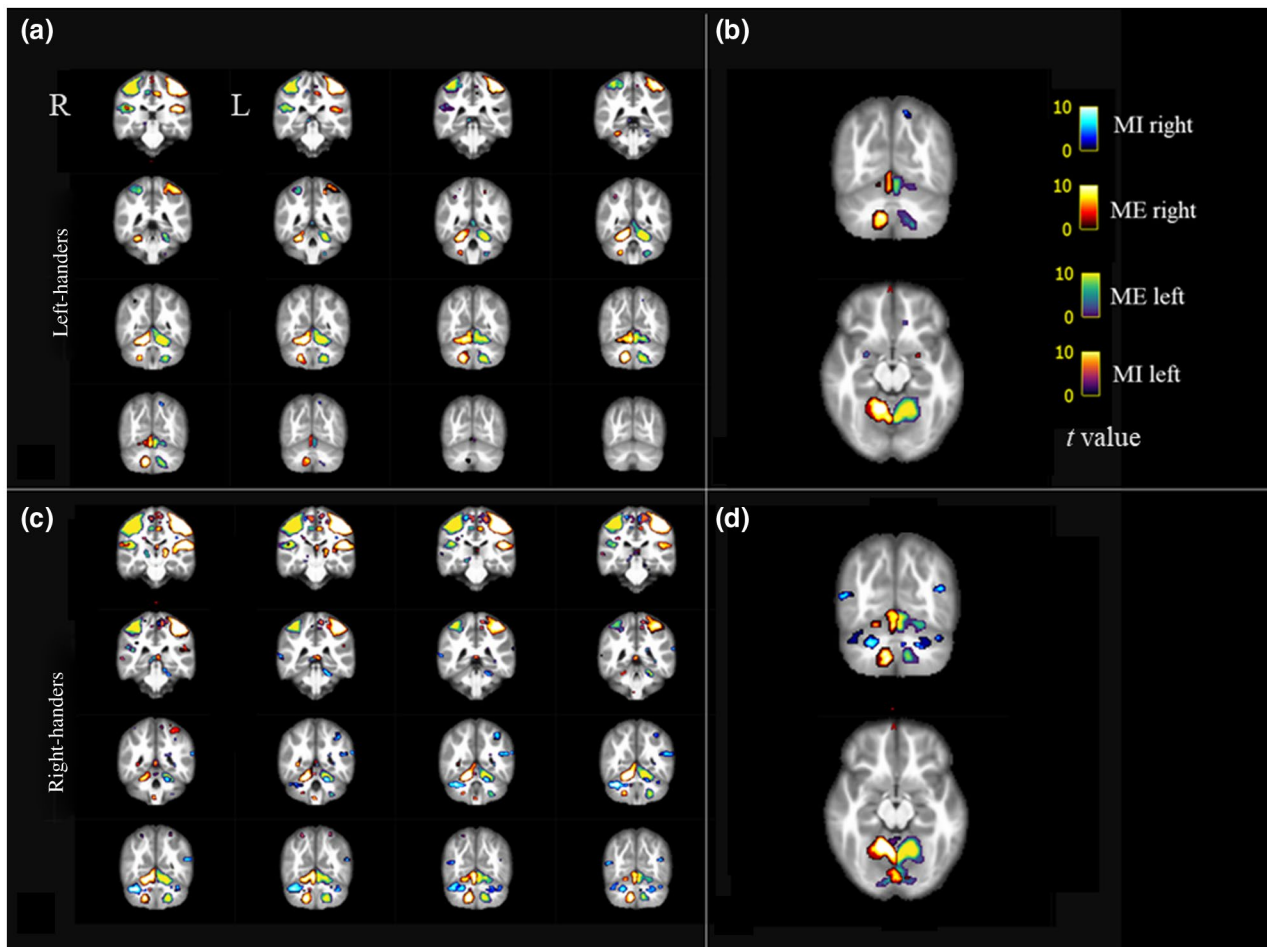
FIGURE 5 Within-group contrasts with focus on the cerebellum. (a,b) Within-group contrasts for the left-handed group (t test, $n = 45$; $p < 0.05$) for MEleft>MIleft and MEright>MIright. (c,d) Within-group contrasts for the right-handed group (t test, $n = 45$; $p < 0.05$) for MEleft>MIleft and MEright>MIright. Suprathreshold (FWE voxel $p < 0.05$) voxels in comparison with fixation for ME right are shown in red, MI right in blue, MEleft in green, and MIleft in purple. Right hemisphere (R) is displayed on the left side and left hemisphere (L) on the right side

lateralized activation over the ipsilateral hemisphere for MI of the non-dominant hand.

The comparison of "both MI" and "fixation" condition revealed for the right-handed group (Figure 3c, blue) maxima suprathreshold activity over the right lingual gyrus and smaller clusters over the left lingual gyrus, middle occipital and inferior occipital gyrus. The left-handed group (Figure 3c, red) showed the maxima locus over the right calcarine gyrus and smaller clusters over the bilateral cerebellum (VI).

Among the ME conditions, significant group effects ($p < 0.005$) were found for the following contrasts, namely MEleft>0 (Figure 3d), MEright>0 (Figure 3e), and MEboth>0 (Figure 3f). In the right-handed group, "left ME" comparison with "fixation" induced a predominantly right-lateralized activation pattern (Figure 3d, blue), with a global peak on the Rolandic operculum, followed by the right calcarine and fusiform gyrus and right cuneus. In the left-handed group, "left ME" comparison with "fixation" (Figure 3d, red) yielded a more spread and bilateral activation pattern, including the cerebellar vermis, on the right hemisphere the highest peak over the superior temporal calcarine, precentral, middle temporal and fusiform gyrus, cerebellum (IX), and IFG (pars triangularis) while for the left hemisphere over the IFG (pars orbitalis), middle and inferior temporal gyrus and MCC.

In the right-handed group, "right ME" comparison with "fixation" (Figure 3e, blue) induced a predominantly left-lateralized activation pattern over the cerebellum (VI), calcarine and posterior-medial frontal gyrus. Also, for this contrast, the left-handed group yielded a more spread and bilateral activation pattern, including for the right hemisphere the superior occipital and temporal gyrus, cerebellum (VI) fusiform, and lingual gyrus, while for the left hemisphere over the calcarine and lingual and middle orbital gyrus and cerebellum (III). The direct comparison of these two contrasts revealed a different pattern for the two groups, showing a bilateral activation for ME of both the dominant and non-dominant-hands in left-handers and a more lateralized activation over the contralateral hemisphere for ME of both the dominant and non-dominant hands for right-handers.

The comparison of "both ME" and "fixation" condition revealed for the right-handed group (Figure 5f, blue) maxima suprathreshold activity over the right lingual and calcarine gyrus. The left-handed group (Figure 3f, red) showed the maxima locus over the bilateral cerebellum (VI-crus 1) and left pre- and postcentral gyrus.

3.2.2 | Within-group

Among ME conditions, significant within-group effects ($p < 0.005$) were found for the contrast MEleft>MEright for both the groups, showing contralateral involvement of the cortical motor areas and ipsilateral cerebellum (for a complete description, see Extended Data, Tables 4.3 and 4.4).

Among MI conditions, significant within-group effects ($p < 0.005$) were found for the contrast MIleft>MIright for both the groups. In the left-handed group (Figure 4a), right-hand MI (blue) induced a bilateral activation over the calcarine gyrus while for left-hand MI (red), over the bilateral lingual gyrus. A result of interest is that for both the conditions, the highest peak was found over the ipsilateral hemisphere for MI task.

In the right-handed group (Figure 4b), both right- and left-hand MI induced a bilateral activation over the lingual gyrus with the highest peak over the ipsilateral hemisphere for MI task.

3.2.3 | The cerebellum

The within-group comparison of MI and ME for the conditions of right and left hands with a specific focus on the cerebellum is described below.

Left-handers' (Figure 5; panel a,b) within-group analysis (i.e., MEleft>MIleft and MEright>MIright) showed for "left ME" (green) significant pattern (FWE voxel $p < 0.05$) over the cerebellar vermis (4/5), and left cerebellum (IV-V-VIII) while "right ME" (red) over the right cerebellum (VIII). No significant activity was found over the cerebellum for the reverse contrasts (i.e., MEleft<MIleft and MEright<MIright).

Right-handers' (Figure 5; panel C, D) within-group analysis (i.e., MEleft>MIleft and MEright>MIright) showed for "left ME" (green) significant pattern (FWE voxel $p < 0.05$) over the cerebellar vermis (3) and left cerebellum (IV-V-VIII) while "right ME" (red) over the cerebellar vermis (6), right (IX) and left (Crus1) cerebellum. The reverse contrasts (i.e., MEleft<MIleft and MEright<MIright) revealed for "left MI" (purple) significant pattern (FWE voxel $p < 0.05$) over the cerebellar vermis (3) and right cerebellum (IX) while for "right MI" (blue) over the right (VIII) and left (VIII; Crus 2) cerebellum.

4 | DISCUSSION

It is widely recognized that MI and ME rely on partly overlapping mechanisms. However, the exact nature of their relationship still lacks a proper definition. More in detail, it is not well understood how MI differs across individuals based on their experience. With specific regard to hand movements, the question is whether MI neural correlates vary between right and left-handers and to which extent this difference is resembling the one found for ME. Several neuroimaging studies have addressed this issue, finding mixed results (Decety, 1996; Fitts & Peterson, 1964; Jeannerod, 1994, 1995; Viviani & Schneider, 1991). The majority corroborate the hypothesis that right and left-handed individuals show different patterns of brain activity during MI tasks. Although these differences are well recognized, most of the fMRI studies concern only right-handed participants (Ehrsson et al., 2003; Szameitat et al., 2007a, 2007b).

To the best of our knowledge, there is less research directly investigating the effects of handedness in both right and left-handed individuals at cortical and subcortical level. One recent study (Willems et al., 2009) directly investigates handedness effects on MI in both the groups, but within the relationship to the more abstract domain of language (i.e., imagination after action/non-action verb presentation). Indeed, Willems et al. (2009) investigated MI in both right and left-handers, using as stimuli Dutch verbs, expressing concrete actions (half related and half not related to manual actions). This is a fundamental difference from our study where stimuli were pictures, and there was no involvement of language domain. The study of Grabowska et al. (2012) includes both right and left-handers but it was focused on ME only (i.e., flexion/extension of the index finger, successive finger-thumb opposition). The same can be said for the study of Tzourio-Mazoyer et al. (2021). Furthermore, no one of the mentioned studies investigated the difference between groups for MI and ME of both hands. Lastly, our comparison includes an extensive analysis of the cerebellar activity.

To achieve a deeper understanding of handedness effects on MI in both right and left-hander individuals, the present study used functional magnetic resonance imaging (fMRI) to compare neural correlates associated with the execution and imagination of a simple task (i.e., squeezing a ball) with the dominant, non-dominant, and both hands. More in detail, given the superior role of the kinesthetic content of MI in recruiting the sensorimotor system, we asked participants to precisely concentrate on the feeling experienced. A further question we addressed was whether individual hand dominance assessed using the EHI (Oldfield, 1971) was associated with the HDT (Steingrüber & Lienert, 1971). In such a way, we investigated whether there was a correlation between handedness self-report and performance-based assessment.

Overall, in our study, we showed a partial spatial overlap of MI and ME in motor and premotor areas, sensory cortices, and cerebellum. The results of the performed analysis confirmed our research hypothesis. Indeed, handedness significantly impacts the neural correlates of MI for both the dominant, non-dominant, and both hand tasks.

Group differences for MI were found for the left and right-hand tasks, revealing a similar pattern for the two groups with a bilateral

activation for MI of the dominant hand. Indeed, for this contrast, both groups recruited the right calcarine gyrus and left occipital gyrus. On the contrary, a more lateralized activation was found for both groups over the ipsilateral occipital lobe for MI of the non-dominant hand. A result of interest is that both right and left-handers showed maxima suprathreshold activation for both hands MI over the right occipital lobe.

The occipital lobe is the site of visual processes control where the primary visual cortex (V1) is mainly located in the calcarine sulcus and the lingual gyrus is responsible for letter processing and encoding visual memories. Since the stimuli we used were pictures of the hand, the activation of such areas for MI is explained by their visual processing. Furthermore, the activation of the lingual gyrus could represent the retrieval of the sensation and feelings associated with the movements, which was what we required for kinesthetic MI.

When compared these results with the ones of ME, a different pattern was found. Group differences for ME were found for the left and right-hand movement compared to fixation, revealing a bilateral activation for ME of both the dominant and non-dominant hands in left-handers and a more lateralized activation over the contralateral hemisphere for ME of both the dominant and non-dominant hands for right-handers. Both hand ME showed maxima suprathreshold activation for right-handers over the right occipital lobe while left-handers recruited the bilateral cerebellum and left motor and sensory cortices. These results are in line with previous findings supporting the hypothesis that left-handers recruit a more spread bilateral network for ME tasks (Jäncke, 1996; Solodkin et al., 2004).

Furthermore, the present study demonstrated that the non-dominant precentral gyrus was active in both right- and left-handers for MI of both dominant and non-dominant hands. On the other side, the dominant precentral gyrus was active only in right-handers and only for MI of the dominant hand. A previous study (Perruchoud et al., 2018) showed that the stimulation of the dominant precentral gyrus played a causal involvement in MI. Together with our findings, it could be proposed that the activation of a region causally involved in MI, such as the dominant precentral gyrus (Perruchoud et al., 2018), can be further correlated with handedness. Indeed, the activation of the precentral gyrus was present in right-handers and specifically for MI of the dominant hand, but not in left-handers.

With regard to within-group analysis of MEleft>MEright, we replicate previous findings (Baraldi et al., 1999; Kim et al., 1993; Singh et al., 1998) for both the groups, showing controlateral involvement of the cortical motor areas and ipsilateral cerebellum.

Among MI conditions, significant within-group effects ($p < 0.05$) were found for the contrast MIleft>MIright for both the groups, showing bilateral activation over the occipital cortex. A result of interest is that for both the conditions and groups, the highest peak was found over the ipsilateral hemisphere for MI task. Differentially from previous studies with MI on right-handers only, we did not find a significant difference between MI of the dominant and non-dominant hands in motor and sensorimotor cortices (Szameitat et al., 2007b; Zhang et al., 2017). These differences could be caused by the different

paradigms used and MI modalities which were not controlled for all these studies.

A further result of special interest is the analysis of the cerebellum activity in ME and MI when compared the execution of the task with the same hand (i.e., MEleft>MIleft and MEright>MIright). Our results showed that overt movements (i.e., MEleft and MEright) in comparison to MI activated ipsilateral cerebellar lobules IV-VI and VIII, which are the sites of the cerebellar homunculus (Mottolese et al., 2013). This pattern was found in both right and left-handers.

Differentially, cerebellar involvement in MI was found to be different between right and left-handers. If in the former, left MI led to significant activity (FWE voxel $p < 0.05$) over the cerebellar vermis (3) and right cerebellum (IX) while right MI over the right (VIII) and left (VIII; Crus 2) cerebellum; no significant activity was found for left-handers. More in detail, the recruitment of the posterior cerebellum (lobe IX) found in right-handers is in accordance with previous findings (Lotze et al., 1999) suggesting the role of such area in the inhibition of ME. Additionally, the cerebellar Crus 2 is considered to be involved in higher order cognition functions.

Furthermore, the between-task analysis revealed that MI, in both groups for both right and left hand, showed the maxima activation over the left posterior medial frontal cortex (pMFC) which is the site of SMA. This is in accordance with the meta-analysis of Hétu et al. (2013), which showed this area as the peak locus for MI. Additionally, this is in line with the study of Guillot et al. (2014), comparing KMI to VMI neural correlates. Their results showed (Guillot et al., 2014) for kinesthetic imagery activity over motor-related regions including contralateral M1, PMC, SMA, cerebellum, basal ganglia, and in the inferior parietal cortex. In contrast, during visual imagery, they observed more activity in occipital regions and superior parietal lobule, including the precuneus. It is to note that in our study, both groups showed left pMFC involvement despite the hand imagined. Moreover, in right-handers, a more bilateral network was found for MI compared to ME; while left-handers showed suprathreshold activity mainly only in the left hemisphere.

Another important aspect of our study is the assessment of handedness. Despite the fact that most of the studies involve only one measurement (e.g., EDI), we decided to include both a self-report (i.e., EHI; Oldfield, 1971) and a behavioral test (i.e., HDT; Steingrüber and Lienert (1971)) in order to define more precisely the two groups. According to the literature, both measurements are reliable, but a single-hand performance measure did not always correctly classify an individual hand dominance (Brown et al., 2004; Corey et al., 2001). On the other side, the combination of results from different tasks was predictive of hand preference (Corey et al., 2001). Our analysis showed a strong correlation ($r = 0.866$) between these two measurements. One aspect of interest visible in the correlation plot is that there are a few participants whose self-report score differentiates from the behavioral task (e.g., on the EDI they score right and the performance of the HDT defined them more left-handers or vice versa). Since they are only a few and the correlation between the two questionnaires is

strong, we suppose that our study has a good distinction between the right and left-handed participants.

Some limitations of our findings should also be noted. First of all, the lack of a comprehensive analyses of potential gender difference. Being aware of its importance, we run a pattern recognition analysis between male and female (See Figure 9 in the Extended Data). Results show a total accuracy rather poor (53.19%). Thus, we conclude that there is no a strong pattern distinction between males and females and that sex did not play a major influence on our results. Nevertheless, we do think that further investigation is needed to address a comprehensive analysis of sex influence on both behavioral and neuroimaging data. Second, our participants were explicitly trained to focus on the kinesthetic feelings and consequences of the actions that they imagined. This is different compared to visual-MI in which participants are instructed to focus on the visual aspects of MI. In order to have a feedback about the engagement of such a modality, we asked our participants to fill the VMIQ-2. Our results ranged from low to high with no statistical difference between the two groups. Thus, we could assume that our sample MI ability ranges from low to high level of MI. Being aware of the subjectivity of this measurement, the interpretation of such results is hence speculative. Additionally, future studies should include muscular activity measurements (e.g., EMG) to record possible muscle activation during the MI tasks.

5 | CONCLUSION

To sum up, the present study provides for the first time an extensive comparison between right-and left-handers' neural correlates for ME and MI tasks with the dominant, non-dominant, and both hands.

Our results replicated previous findings on ME, showing contralateral involvement of the cortical motor areas and ipsilateral cerebellum. We also replicated differences between groups, showing that left-handers recruit a spread bilateral network while in right-handers, activity is more lateralized.

Furthermore, for the first time, we highlighted different patterns of the cerebellum activity for ME and MI. We showed that in both groups, overt movements (i.e., MEleft and MEright) activated ipsilateral cerebellar lobules IV–VI and VIII, considered to be the sites of the cerebellar homunculus. Differentially, for MI, right-handers showed the involvement of the posterior cerebellum, considered to be involved in movement inhibition and higher order functions. No significant activity was found for left-handers.

According to our hypothesis, right and left-handers showed different neural correlates of MI. A result of interest is that for both the conditions (i.e., leftMI and rightMI) and groups, the highest peak was found over the ipsilateral hemisphere for MI task. Such differences do not correspond to the ones found for ME. Difference in activation with previous findings can be explained by the different methodology used such as the paradigm, the complexity of the task and the control for the MI modality. Lastly, a different pattern between groups was identified for the cerebellar activity in MI.

Our findings could be used to exploit new clinical assessments and treatment approaches. In the context of brain–computer interface, MI is a valuable approach used with different techniques and clinical populations (see Frolov et al. (2017); Vourvopoulos et al. (2019); Khan et al. (2020) for a review). In conclusion, we do think the present study could be used to ameliorate rehabilitation planning (e.g., personalized treatment) and clinical assessments.

A question that remains unaddressed is whether this difference is present at the level of brain connectivity. In our paradigm, we indeed include the acquisition of DTI data for future analysis, disentangling this issue and further clarifying the impact of handedness on brain circuit development.

ORCID
Monica Crotti https://orcid.org/0000-0003-3206-2006
Karl Koschutnig https://orcid.org/0000-0001-6234-0498
Selina Christin Wriessnegger https://orcid.org/0000-0003-4345-7310

REFERENCES
Annett, J. (1995). Motor imagery: Perception or action? *Neuropsychologia*, *33*(11), 1395–1417. https://doi.org/10.1016/0028-3932(95)00072-B

Baraldi, P., Porro, C. A., Serafini, M., Panoni, G., Murari, C., Corazza, R., & Nichelli, P. (1999). Bilateral representation of sequential finger movements in human cortical areas. *Neuroscience Letters*, *269*(2), 95–98. https://doi.org/10.1016/S0304-3940(99)00433-4

Bostan, A. C., Dum, R. P., & Strick, P. L. (2013). Cerebellar networks with the cerebral cortex and basal ganglia. *Trends in Cognitive Sciences*, *17*(5), 241–254.

Brown, S. G., Roy, E. A., Rohr, L. E., Snider, B. R., & Bryden, P. J. (2004). Preference and performance measures of handedness.

Brain and Cognition, *55*(2), 283–285. https://doi.org/10.1016/j.bandc.2004.02.010

Buckner, R. L. (2013). The cerebellum and cognitive function: 25 years of insight from anatomy and neuroimaging. *Neuron*, *80*(3), 807–815. https://doi.org/10.1016/j.neuron.2013.10.044

Buckner, R. L., Krienen, F. M., Castellanos, A., Diaz, J. C., & Yeo, B. T. (2011). The organization of the human cerebellum estimated by intrinsic functional connectivity. *Journal of Neurophysiology*, *106*(5), 2322–2345. https://doi.org/10.1152/jn.00339.2011

Casasanto, D. (2009). Embodiment of abstract concepts: Good and bad in right-and left-handers. *Journal of Experimental Psychology: General*, *138*(3), 351–367. https://doi.org/10.1037/a0015854

Cattaneo, Z., & Silvanto, J. (2015). Mental imagery: Visual cognition. In J. D. Wright (Ed.), *International encyclopedia of the social & behavioral sciences* (2nd ed., pp. 220–227). Elsevier. https://doi.org/10.1016/B978-0-08-097086-8.57024-X; https://www.sciencedirect.com/science/article/pii/B978008097086857024X

Corey, D. M., Hurley, M. M., & Foundas, A. L. (2001). Right and left handedness defined: A multivariate approach using hand preference and hand performance measures. *Cognitive and Behavioral Neurology*, *14*(3), 144–152.

Dassonville, P., Zhu, X.-H., Ugurbil, K., Kim, S.-G., & Ashe, J. (1997). Functional activation in motor cortex reflects the direction and the degree of handedness. *Proceedings of the National Academy of Sciences of the United States of America*, *94*(25), 14015–14018. https://doi.org/10.1073/pnas.94.25.14015

Decety, J. (1996). Do imagined and executed actions share the same neural substrate? *Cognitive Brain Research*, *3*(2), 87–93. https://doi.org/10.1016/0926-6410(95)00033-X

Ehrsson, H. H., Geyer, S., & Naito, E. (2003). Imagery of voluntary movement of fingers, toes, and tongue activates corresponding body-part-specific motor representations. *Journal of Neurophysiology*, *90*(5), 3304–3316. https://doi.org/10.1152/jn.01113.2002

Eickhoff, S. B., Stephan, K. E., Mohlberg, H., Grefkes, C., Fink, G. R., Amunts, K., & Zilles, K. (2005). A new SPM toolbox for combining probabilistic cytoarchitectonic maps and functional imaging data. *NeuroImage*, *25*(4), 1325–1335. https://doi.org/10.1016/j.neuroimage.2004.12.034

Esteban, O., Blair, R., Markiewicz, C. J., Berleant, S. L., Moodie, C., Ma, F., Isik, A. I., Erramuzpe, A., Kent, J. D., Goncalves, M., DuPre, E., Sitek, K. R., Gomez, D. E. P., Lurie, D. J., Ye, Z., Poldrack, R. A., & Gorgolewski, K. J. (2018). fMRIPrep. *Software*. https://doi.org/10.5281/zenodo.852659

Esteban, O., Markiewicz, C., Blair, R. W., Moodie, C., Isik, A. I., Erramuzpe Aliaga, A., Kent, J., Goncalves, M., DuPre, E., Snyder, M., Oya, H., Ghosh, S., Wright, J., Durnez, J., Poldrack, R., & Gorgolewski, K. J. (2018). fMRIPrep: A robust preprocessing pipeline for functional MRI. *Nature Methods*, *16*(1), 111–116. https://doi.org/10.1038/s41592-018-0235-4

Fitts, P. M., & Peterson, J. R. (1964). Information capacity of discrete motor responses. *Journal of Experimental Psychology*, *67*(2), 103–112. https://doi.org/10.1037/h0045689

Frolov, A. A., Mokienko, O., Lyukmanov, R., Biryukova, E., Kotov, S., Turbina, L., Nadareyshvily, G., & Bushkova, Y. (2017). Post-stroke rehabilitation training with a motor-imagery-based brain-computer interface (BCI)-controlled hand exoskeleton: A randomized controlled multicenter trial. *Frontiers in Neuroscience*, *11*. https://doi.org/10.3389/fnins.2017.00400

Gao, Q., Duan, X., & Chen, H. (2011). Evaluation of effective connectivity of motor areas during motor imagery and execution using conditional Granger causality. *NeuroImage*, *54*(2), 1280–1288. https://doi.org/10.1016/j.neuroimage.2010.08.071

Gentilucci, M., Daprati, E., & Gangitano, M. (1998). Right-handers and left-handers have different representations of their own hand. *Cognitive Brain Research*, *6*(3), 185–192. https://doi.org/10.1016/S0926-6410(97)00034-7

Gerardin, E. (2000). Partially overlapping neural networks for real and imagined hand movements. *Cerebral Cortex*, *10*(11), 1093–1104. https://doi.org/10.1093/cercor/10.11.1093

Gorgolewski, K., Burns, C. D., Madison, C., Clark, D., Halchenko, Y. O., Waskom, M. L., & Ghosh, S. (2011). Nipype: A flexible, lightweight and extensible neuroimaging data processing framework in Python. *Frontiers in Neuroinformatics*, *5*, 13. https://doi.org/10.3389/fninf.2011.00013

Grabowska, A., Gut, M., Binder, M., Forsberg, L., Rymarczyk, K., & Urbanik, A. (2012). Switching handedness: fMRI study of hand motor control in right-handers, left-handers and converted left-handers. *Acta Neurobiologiae Experimentalis (Wars)*, *72*(4), 439–451.

Guillot, A., Collet, C., Nguyen, V. A., Malouin, F., Richards, C., & Doyon, J. (2008). Functional neuroanatomical networks associated with expertise in motor imagery. *NeuroImage*, *41*(4), 1471–1483. https://doi.org/10.1016/j.neuroimage.2008.03.042

Guillot, A., di Rienzo, F., & Collet, C. (2014). The neurofunctional architecture of motor imagery. In *Advanced brain neuroimaging topics in health and disease-methods and applications* (pp. 433–456). https://doi.org/10.5772/58270

Hanakawa, T., Immisch, I., Toma, K., Dimyan, M. A., van Gelderen, P., & Hallett, M. (2003). Functional properties of brain areas associated with motor execution and imagery. *Journal of Neurophysiology*, *89*(2), 989–1002. https://doi.org/10.1152/jn.00132.2002

Hétu, S., Grégoire, M., Saimpont, A., Coll, M. P., Eugène, F., Michon, P. E., & Jackson, P. L. (2013). The neural network of motor imagery: An ALE meta-analysis. *Neuroscience & Biobehavioral Reviews*, *37*(5), 930–949. https://doi.org/10.1016/j.neubiorev.2013.03.017

Jäncke, L. (1996). The hand performance test with a modified time limit instruction enables the examination of hand performance asymmetries in adults. *Perceptual and Motor Skills*, *82*(3), 735–738. https://doi.org/10.2466/pms.1996.82.3.735

Jeannerod, M. (1994). The representing brain: Neural correlates of motor intention and imagery. *Behavioral and Brain Sciences*, *17*(2), 187–202. https://doi.org/10.1017/S0140525X00034026

Jeannerod, M. (1995). Mental imagery in the motor context. *Neuropsychologia*, *33*(11), 1419–1432. https://doi.org/10.1016/0028-3932(95)00073-C

Jeannerod, M. (2001). Neural simulation of action: A unifying mechanism for motor cognition. *NeuroImage*, *14*(1), S103–S109. https://doi.org/10.1006/nimg.2001.0832

Kawashima, R., Inoue, K., Sato, K., & Fukuda, H. (1997). Functional asymmetry of cortical motor control in left-handed subjects. *NeuroReport*, *8*(7), 1729–1732. https://doi.org/10.1097/00001756-199705060-00032

Khan, M. A., Das, R., Iversen, H. K., & Puthusserypady, S. (2020). Review on motor imagery based BCI systems for upper limb post-stroke neurorehabilitation: From designing to application. *Computers in Biology and Medicine*, *123*, 103843. https://doi.org/10.1016/j.compbiomed.2020.103843

Kim, S., Ashe, J., Hendrich, K., Ellermann, J., Merkle, H., Ugurbil, K., & Georgopoulos, A. (1993). Functional magnetic resonance imaging of motor cortex: Hemispheric asymmetry and handedness. *Science*, *261*(5121), 615–617. https://doi.org/10.1126/science.8342027

Lotze, M., Montoya, P., Erb, M., Hülsmann, E., Flor, H., Klose, U., Birbaumer, N., & Grodd, W. (1999). Activation of cortical and cerebellar motor areas during executed and imagined hand movements: An fMRI study. *Journal of Cognitive Neuroscience*, *11*(5), 491–501. https://doi.org/10.1162/089892999563553

Michelon, P., Vettel, J. M., & Zacks, J. M. (2006). Lateral somatotopic organization during imagined and prepared movements. *Journal of Neurophysiology*, *95*(2), 811–822. https://doi.org/10.1152/jn.00488.2005

Mottolese, C., Richard, N., Harquel, S., Szathmari, A., Sirigu, A., & Desmurget, M. (2013). Mapping motor representations in the human

cerebellum. *Brain*, *136*(1), 330–342. https://doi.org/10.1093/brain/aws186

Nico, D. (2004). Left and right hand recognition in upper limb amputees. *Brain*, *127*(1), 120–132. https://doi.org/10.1093/brain/awh006

Oldfield, R. C. (1971). The assessment and analysis of handedness: The Edinburgh inventory. *Neuropsychologia*, *9*(1), 97–113. https://doi.org/10.1016/0028-3932(71)90067-4

Perruchoud, D., Fiorio, M., Cesari, P., & Ionta, S. (2018). Beyond variability: Subjective timing and the neurophysiology of motor cognition. *Brain Stimulation*, *11*(1), 175–180. https://doi.org/10.1016/j.brs.2017.09.014

Perruchoud, D., Michels, L., Piccirelli, M., Gassert, R., & Ionta, S. (2016). Differential neural encoding of sensorimotor and visual body representations. *Scientific Reports*, *6*(1), 1–10. https://doi.org/10.1038/srep37259

Porro, C. A., Francescato, M. P., Cettolo, V., Diamond, M. E., Baraldi, P., Zuiani, C., Bazzocchi, M., & di Prampero, P. E. (1996). Primary motor and sensory cortex activation during motor performance and motor imagery: A functional magnetic resonance imaging study. *Journal of Neuroscience*, *16*(23), 7688–7698. https://doi.org/10.1523/JNEUROSCI.16-23-07688.1996

Rijntjes, M., Dettmers, C., Büchel, C., Kiebel, S., Frackowiak, R. S. J., & Weiller, C. (1999). A blueprint for movement: Functional and anatomical representations in the human motor system. *The Journal of Neuroscience*, *19*(18), 8043–8048. https://doi.org/10.1523/jneurosci.19-18-08043.1999

Roth, M., Decety, J., Raybaudi, M., Massarelli, R., Delon-Martin, C., Segebarth, C., Morand, S., Gemignani, A., Décorps, M., & Jeannerod, M. (1996). Possible involvement of primary motor cortex in mentally simulated movement: A functional magnetic resonance imaging study. *NeuroReport*, *7*(7), 1280–1284. https://doi.org/10.1097/00001756-199605170-00012

Sakai, K., Hikosaka, O., Miyauchi, S., Sasaki, Y., Fujimaki, N., & Pütz, B. (1999). Presupplementary motor area activation during sequence learning reflects visuo-motor association. *Journal of Neuroscience*, *19*(10), RC1. https://doi.org/10.1523/JNEUROSCI.19-10-j0002.1999

Schrouff, J., Rosa, M. J., Rondina, J. M., Marquand, A. F., Chu, C., Ashburner, J., Phillips, C., Richiardi, J., & Mourão-Miranda, J. (2013). PRoNTo: Pattern recognition for neuroimaging toolbox. *Neuroinformatics*, *11*(3), 319–337. https://doi.org/10.1007/s12021-013-9178-1

Schultz, A. (2017). *GLM flex fast2*. http://mrtools.mgh.harvard.edu/index.php?title=GLM_Flex_Fast2

Shenton, J. T., Schwoebel, J., & Coslett, H. B. (2004). Mental motor imagery and the body schema: Evidence for proprioceptive dominance. *Neuroscience Letters*, *370*(1), 19–24. https://doi.org/10.1016/j.neulet.2004.07.053

Singh, L. N., Higano, S., Takahashi, S., Kurihara, N., Furuta, S., Tamura, H., Shimanuki, Y., Mugikura, S., Fujii, T., Yamadori, A., Sakamoto, M., & Yamada, S. (1998). Comparison of ipsilateral activation between right and left handers. *NeuroReport*, *9*(8), 1861–1866. https://doi.org/10.1097/00001756-199806010-00036

Solodkin, A., Hlustik, P., Chen, E. E., & Small, S. L. (2004). Fine modulation in network activation during motor execution and motor imagery. *Cerebral Cortex*, *14*(11), 1246–1255. https://doi.org/10.1093/cercor/bhh086

Spunt, B. (2016). *spunt/bspmview: BSPMVIEW v. 20161108*. Zenodo.

Steingrüber, H.-J., & Lienert, G. A. (1971). *Hand-dominanz-test: HDT*. Verlag für Psychologie, Hogrefe.

Stephan, K. M., & Frackowiak, R. S. J. (1996). Motor imagery—Anatomical representation and electrophysiological characteristics. *Neurochemical Research*, *21*(9), 1105–1116. https://doi.org/10.1007/BF02532421

Stoodley, C. J., Valera, E. M., & Schmahmann, J. D. (2012). Functional topography of the cerebellum for motor and cognitive tasks: An fMRI study. *NeuroImage*, *59*(2), 1560–1570. https://doi.org/10.1016/j.neuroimage.2011.08.065

Szameitat, A. J., Shen, S., & Sterr, A. (2007a). Effector-dependent activity in the left dorsal premotor cortex in motor imagery. *European Journal of Neuroscience*, *26*(11), 3303–3308. https://doi.org/10.1111/j.1460-9568.2007.05920.x

Szameitat, A. J., Shen, S., & Sterr, A. (2007b). Motor imagery of complex everyday movements. An fMRI study. *NeuroImage*, *34*(2), 702–713. https://doi.org/10.1016/j.neuroimage.2006.09.033

Tournier, J.-D., Smith, R., Raffelt, D., Tabbara, R., Dhollander, T., Pietsch, M., Christiaens, D., Jeurissen, B., Yeh, C.-H., & Connelly, A. (2019). MRtrix3: A fast, flexible and open software framework for medical image processing and visualisation. *NeuroImage*, *202*, 116137. https://doi.org/10.1016/j.neuroimage.2019.116137

Tzourio-Mazoyer, N., Labache, L., Zago, L., Hesling, I., & Mazoyer, B. (2021). Neural support of manual preference revealed by BOLD variations during right and left finger-tapping in a sample of 287 healthy adults balanced for handedness. *Laterality*, 1–23. https://doi.org/10.1080/1357650x.2020.1862142

van der Zwaag, W., Kusters, R., Magill, A., Gruetter, R., Martuzzi, R., Blanke, O., & Marques, J. P. (2013). Digit somatotopy in the human cerebellum: A 7 T fMRI study. *NeuroImage*, *67*, 354–362. https://doi.org/10.1016/j.neuroimage.2012.11.041

Vigneswaran, G., Philipp, R., Lemon, R. N., & Kraskov, A. (2013). M1 corticospinal mirror neurons and their role in movement suppression during action observation. *Current Biology*, *23*(3), 236–243. https://doi.org/10.1016/j.cub.2012.12.006

Viviani, P., & Schneider, R. (1991). A developmental study of the relationship between geometry and kinematics in drawing movements. *Journal of Experimental Psychology: Human Perception and Performance*, *17*(1), 198–218. https://doi.org/10.1037/0096-1523.17.1.198

Vourvopoulos, A., Jorge, C., Abreu, R., Figueiredo, P., Fernandes, J.-C., & Bermúdez i Badia, S. (2019). Efficacy and brain imaging correlates of an immersive motor imagery BCI-driven VR system for upper limb motor rehabilitation: A clinical case report. *Frontiers in Human Neuroscience*, *13*. https://doi.org/10.3389/fnhum.2019.00244

Willems, R. M., Toni, I., Hagoort, P., & Casasanto, D. (2009). Body-specific motor imagery of hand actions: Neural evidence from right- and left-handers. *Frontiers in Human Neuroscience*, *3*, 39. https://doi.org/10.3389/neuro.09.039.2009

Wriessnegger, S. C., Steyrl, D., Koschutnig, K., & Muller-Putz, G. R. (2014). Short time sports exercise boosts motor imagery patterns: Implications of mental practice in rehabilitation programs. *Frontiers in Human Neuroscience*, *8*, 469. https://doi.org/10.3389/fnhum.2014.00469

Zhang, R., Yan, Y., Hu, Y., Shi, L., & Wan, H. (2017, October). Eeg function network analysis of left and right hand motor imagery. In *2017 Chinese Automation Congress (CAC)* (pp. 346–350). https://doi.org/10.1109/CAC.2017.8242790

APPENDIX

EXTENDED DATA

CODE

Vividness of Movement Imagery Questionnaire-2

Name: Age:

Gender: Sport:

Movement imagery refers to the ability to imagine a movement. The aim of this questionnaire is to determine the vividness of your Kinaesthetic movement imagery.

The items of the questionnaire are designed to bring certain images to your mind. Try to obtain them by feeling yourself do the movement (Kinaesthetic imagery).

Please try to be concentrated on the feeling experienced and NOT to use an external point of view such watching yourself performing the movement (External Visual Imagery) or an internal point of view, as if you were looking out through your own eyes whilst performing the movement (Internal Visual Imagery).

You are asked to rate the vividness of each item by reference to the 5-point scale. After each item, circle the appropriate number in the boxes provided.

For all items please have your eyes CLOSED.

Think of each of the following acts that appear on the next page, and classify the images according to the degree of clearness and vividness as shown on the RATING SCALE.

RATING SCALE. The image aroused by each item might be:
Perfectly clear and as vivid (as normal vision or feel of movement) ....RATING 1
Clear and reasonably vivid   ....RATING 2
Moderately clear and vivid   ....RATING 3
Vague and dim   ....RATING 4
No image at all, you only "know" that you are thinking of the skill........... RATING 5

Item	Feeling yourself do the movement (Kinaesthetic Imagery)				
	Perfectly clear and vivid as normal feel of movement	Clear and reasonably vivid	Moderately clear and vivid	Vague and dim	No image at all, you only know that you are thinking of the skill
1.Walking	1	2	3	4	5
2.Running	1	2	3	4	5
3.Kicking a stone	1	2	3	4	5
4.Bending to pick up a coin	1	2	3	4	5
5.Running up stairs	1	2	3	4	5
6.Jumping sideways	1	2	3	4	5
7.Throwing a stone into water	1	2	3	4	5
8.Kicking a ball in the air	1	2	3	4	5
9.Running downhill	1	2	3	4	5
10.Riding a bike	1	2	3	4	5
11.Swinging on a rope	1	2	3	4	5
12.Jumping off a high wall	1	2	3	4	5

FIGURE 6   Kinesthetic part of the Vividness of Movement Imagery Questionnaire (VMIQ-2). Example of the kinesthetic part of the VMIQ-2 which was administered to each participant to obtain a self-report index of participants' imagery ability. On the left, the name, age, gender, and information about sport played by the participant were reported before reading the instructions. Participants had to rate on a scale between 1 (low) and 5 (high) how clear and vivid was feeling himself/herself doing the movement of the 12 items (i.e., actions) reported on the right side. The total score is calculated by the sum of the 12 items

FIGURE 7 COVID symptoms questionnaire. COVID-19 questionnaire which was administered to each participant before entering the laboratory. Seven screening items must be checked as "No" to allow the participant to take part in the study

COVID-19 questionnaire for an MR research exam
MRI Laboratory Graz, Institute for Psychology

Personal data:

Name:		Date of birth:	

In order to carry out the MR research examination, we ask you to answer conscientiously to the following questions within a maximum of 48 hours before your agreed appointment.

Do you currently have or have you had in the past week:

Fever	○ Yes ○ No
Sore throat	○ Yes ○ No
Dry cough	○ Yes ○ No
shortness of breath	○ Yes ○ No
Shortness of breath	○ Yes ○ No
Taste disorders / odor disorders	○ Yes ○ No
Diarrhea / vomiting	○ Yes ○ No

**Is your body temperature 37.5 ° C or more?**

○ Yes	○ No

If you answered YES to any of the points, it is not possible to conduct the research investigation or to enter the laboratory. Otherwise, take the completed and signed questionnaire with you on the agreed date.

If you have specific symptoms, stay at home and call health number 1450 for further clarification.

I confirm that I have read, understood and truthfully answered the questions that concern me.

_____
Date and signature (subject, parents or legal representative)

FIGURE 8 Multi-voxel pattern analysis for motor imagery. Classification analysis based on left and right motor imagery tasks. Black crosses represent motor imagery (MI) of the right hand, and red circles represent MI of the left hand. The dashed line is the cutoff function value between both groups
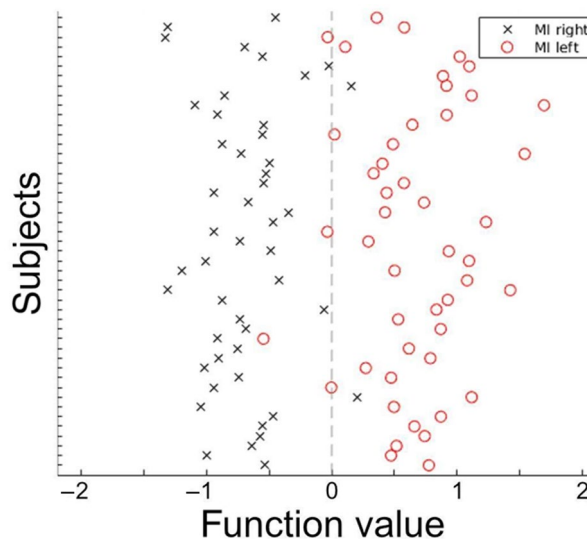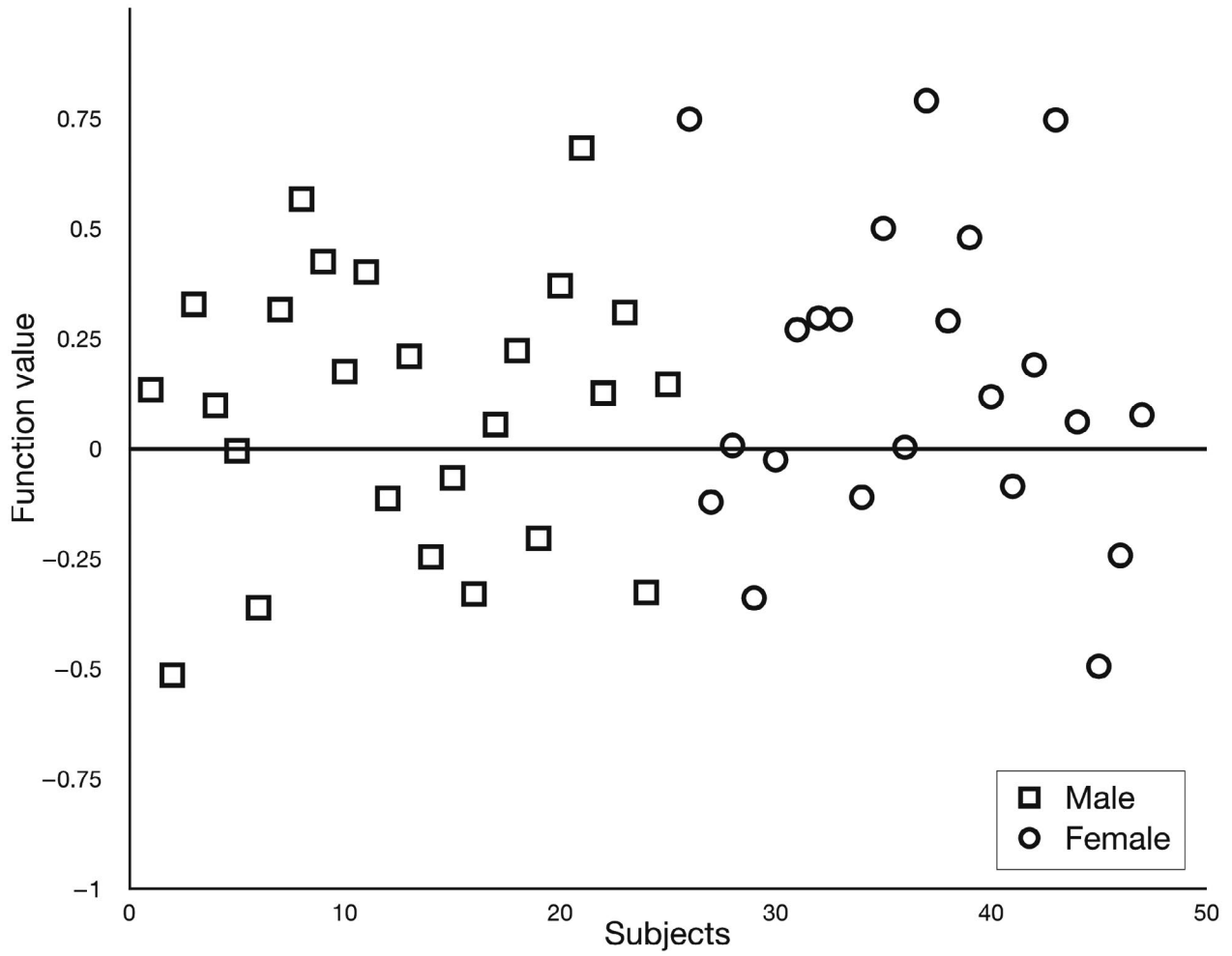
FIGURE 9 Multi-voxel pattern analysis for gender difference. Classification analysis of the motor imagery task (left MI vs. right MI) based on gender difference. Circles represent females and squares represent males. The horizontal line is the cutoff function value between both groups

TABLE 3 GLM-Flex results analysis of main effects and interactions

	Region label	Extent	F-value	MNI coordinates		
				x	y	z
Group			n.s.			
Hand	Precentral_R	21,845	615.045	38	−25	53
	Postcentral_L		548.195	−46	−23	58
	Precentral_L		229.608	−28	−21	69
	Cerebellum_4_5_R	45,126	387.170	19	−50	−23
	Cerebellum_4_5_L		349.282	−19	−50	−21
	Cerebellum_8_L		217.797	−19	−59	−52
	Occipital_Inf_R	728	29.055	27	−97	−10
	Location not in atlas		20.849	17	−106	4
	Precentral_R	232	19.323	60	8	35
	Location not in atlas	175	18.204	8	−30	−41
	Location not in atlas	26	16.193	−23	−37	19
	Cerebellum_Crus2_L	165	16.020	−26	−82	−35
	Cerebellum_Crus2_R	139	14.787	24	−77	−41
	Cerebellum_Crus1_L	29	14.098	−52	−53	−30
	Frontal_Inf_Tri_L	145	13.996	−50	29	2
	Frontal_Inf_Tri_R	63	13.475	56	26	4
	Temporal_Sup_R	78	13.133	62	−17	−3
	Frontal_Sup_Medial_L	26	10.955	−8	38	51
	Temporal_Mid_L	23	10.720	−68	−41	8
	Precentral_L	22	10.419	−61	2	37
	Temporal_Pole_Mid_R	31	10.385	47	6	−32
	Temporal_Mid_L	27	10.319	−55	−1	−26
	Temporal_Mid_L	30	9.275	−52	8	−26
	Temporal_Mid_L	70	9.182	−68	−12	−1
	OFClat_R	25	9.064	45	36	−16
Group × Hand	Temporal_Mid_L	124	15.331	−61	−37	−1
	Cerebellum_6_R	52	14.817	15	−68	−26
	Cingulate_Mid_L	136	14.488	−12	−50	31
	Cingulate_Post_R	136	7.546	4	−44	20
	ACC_sup_L	65	14.157	−7	26	19
	ACC_sub_L	23	13.118	−5	36	−1
	Parietal_Sup_L	162	12.981	−28	−52	56
	Location not in atlas	47	12.606	−44	−21	−10
	Cingulate_Mid_R	25	11.827	4	8	42
	Temporal_Mid_L	31	11.575	−55	0	−26
	Paracentral_Lobule_L	23	11.513	−3	−32	76
	Frontal_Inf_Orb_2_L	72	11.152	−52	42	−5
	Cingulate_Mid_R	89	11.145	6	−23	35
	Precuneus_R	22	10.845	10	−52	22
	Frontal_Inf_Oper_R	44	10.127	53	9	19
	Parietal_Sup_L	35	10.120	−17	−80	55
	Temporal_Mid_R	36	10.079	67	−28	−1
	Temporal_Pole_Mid_R	32	9.408	60	2	−17

TABLE 3 GLM-Flex results analysis of main effects and interactions

TABLE 3 (Continued)

	Region label	Extent	F-value	MNI coordinates		
				x	y	z
	Supp_Motor_Area_L	23	9.365	1	20	64
Condition	Precentral_R	7,304	19.756	38	−23	53
	Rolandic_Oper_R		11.801	44	−25	20
	Postcentral_R		8.501	62	−16	15
	Postcentral_L	4,483	18.997	−46	−26	60
	Cerebellum_4_5_R	8,270	17.412	13	−52	−19
	Cerebellum_6_L		13.756	−14	−57	−14
	Thal_VPL_R		8.587	15	−17	2
	Rolandic_Oper_L	2,476	10.237	−46	−25	20
	Putamen_L		4.842	−32	−10	2
	Rolandic_Oper_L		3.553	−61	0	4
	Cerebellum_8_L	1,190	9.969	−19	−59	−52
	Cerebellum_8_L		5.520	−30	−41	−52
	Location not in atlas		3.632	−5	−79	−46
	Cerebellum_8_R		9.547	13	−62	−50
	Location not in atlas		6.920	4	−46	−59
	Cerebellum_10_R		4.554	22	−35	−46
	Supp_Motor_Area_L	1,634	8.314	1	−17	49
	Cingulate_Mid_L		4.717	−7	0	40
	Location not in atlas	75	4.930	−32	−50	1
	Temporal_Pole_Sup_R	51	4.726	62	6	2
	Location not in atlas	40	4.597	−3	20	4
	Location not in atlas	22	4.568	−10	−23	−39
	Amygdala_L	109	4.503	−17	−1	−21
	Calcarine_R	45	4.473	6	−82	6
	ParaHippocampal_R	28	4.436	29	−25	−28
	Temporal_Inf_L	27	4.373	−34	−1	−34
	Location not in atlas	64	4.263	1	−25	−43
	Frontal_Sup_Medial_R	29	4.097	2	33	60
	Amygdala_R	39	4.042	20	0	−16
Group × Condition	Frontal_Sup_2_L	55	21.954	−28	63	−7
	Frontal_Mid_2_R	31	20.478	35	26	35
	Temporal_Sup_R	40	19.462	67	−35	10
	Cerebellum_6_R	22	19.246	33	−57	−19
	Temporal_Mid_R	34	16.635	69	−44	−1
Hand × Condition	Postcentral_R	12,793	660.965	40	−25	53
	Postcentral_L		563.198	−44	−25	60
	Precentral_R		90.911	24	−25	76
	Cerebellum_4_5_L	8,982	280.097	−19	−50	−25
	Cerebellum_4_5_R		245.597	17	−52	−21
	Cerebellum_4_5_L		122.999	−5	−62	−14
	Rolandic_Oper_L	1,895	81.401	−44	−21	19
	Thal_VPL_L		68.186	−17	−21	6
	Supp_Motor_Area_L	2,191	74.025	−5	−17	49

(Continues)

TABLE 3 (Continued)

	Region label	Extent	F-value	MNI coordinates		
				x	y	z
	Cingulate_Mid_R		17.486	6	0	42
	Rolandic_Oper_R	2,753	72.863	42	−19	19
	Thal_VPL_R		52.589	19	−21	4
	Amygdala_R		33.122	27	−1	−12
	Location not in atlas	108	24.379	4	−46	−61
	Cerebellum_Crus1_R	147	15.910	20	−89	−19
	Putamen_L	84	14.216	−19	8	8
	Location not in atlas	24	13.559	−34	−28	31
	Frontal_Inf_Tri_L	47	12.090	−39	44	10
	OFCpost_L	20	11.005	−23	27	−17
	Location not in atlas	26	10.659	−21	−23	28
Group × Hand × Condition	Occipital_Mid_L	62	16.113	−39	−70	28
	Fusiform_L	63	14.871	−34	−39	−16
	Location not in atlas	82	13.679	−23	42	−3
	OFCant_L	85	11.871	−32	38	−16
	Frontal_Sup_Medial_L	21	10.918	−14	54	4

Note: Region label according to the Anatomy Toolbox atlas (Eickhoff et al., 2005); R = right; L = left. Extent in voxels, *F* values, and MNI coordinates (*x*, *y*, *z*) in Talairach space for each region are displayed.

TABLES 4 **Between-group results**

TABLE 4.1 Between-group result for motor imagery (MI) left hand

MI left hand						
				MNI coordinates		
Contrast	Region label	Extent	t value	x	y	z
left>right-handers	R Calcarine Gyrus	180	9.862	19	−95	10
	L Posterior-Medial Frontal	50	7.516	1	8	55
	L Superior Occipital Gyrus	44	6.908	−16	−95	13
right>left-handers	L Lingual Gyrus	326	−8.664	2	−86	6
	L Cerebellum (Crus 1)	35	−7.270	−32	−80	−17
	L Lingual Gyrus	20	−7.181	−17	−79	−3

Note: Region label according to the Anatomy Toolbox atlas (Eickhoff et al., 2005); R = right; L = left. Extent in voxels, *t* values, and MNI coordinates (*x*, *y*, *z*) in Talairach space for each region are displayed.

TABLE 4.2 Between-group result for motor imagery (MI) right hand

MI right hand						
				MNI coordinates		
Contrast	Region label	Extent	t value	x	y	z
left>right-handers	R Calcarine Gyrus	125	9.005	19	−93	8
right>left-handers	R Calcarine Gyrus	312	−8.957	4	−86	6
	L Lingual Gyrus	86	−7.618	−16	−79	−1
	L Fusiform Gyrus	52	−7.530	−28	−71	−10

Note: Region label according to the Anatomy Toolbox atlas (Eickhoff et al., 2005); R = right; L = left. Extent in voxels, *t* values, and MNI coordinates (*x*, *y*, *z*) in Talairach space for each region are displayed.

TABLE 4.3 Between-group result for motor execution (ME) left hand

ME left hand				MNI coordinates		
Contrast	Region label	Extent	t value	x	y	z
left>right-handers	R Superior Temporal Gyrus	106	9.640	67	−35	13
	R Calcarine Gyrus	117	9.521	19	−91	10
	R Precentral Gyrus	37	8.461	22	−25	76
	R Middle Temporal Gyrus	184	8.195	51	−1	−28
	L IFG (pars orbitalis)	48	7.951	−37	42	−7
	R Cerebellum (IX)	65	7.714	11	−57	−37
	L Middle Temporal Gyrus	292	7.564	−57	2	−26
	L MCC	49	7.449	−7	−26	38
	R Fusiform Gyrus	31	7.342	38	−10	−28
	L Superior Temporal Gyrus	29	7.294	−66	−50	24
	Cerebellar Vermis (3)	34	7.076	−1	−48	−16
	L Inferior Temporal Gyrus	62	6.936	−43	−9	−34
	R IFG (pars triangularis)	49	6.897	44	24	33
	R Cerebellum (VI)	20	6.882	29	−59	−17
	R Posterior-Medial Frontal	21	6.850	17	−16	69
	R Middle Occipital Gyrus	28	6.841	44	−82	15
	R Cerebellum (Crus 2)	22	6.660	49	−55	−35
	R IFG (pars orbitalis)	37	6.363	49	38	−7
right>left-handers	R Rolandic Operculum	46	−8.785	58	−16	20
	R Calcarine Gyrus	364	−7.777	6	−82	15
	L Inferior Temporal Gyrus	33	−7.681	−39	−37	−8
	L Cuneus	29	−7.228	−7	−93	24
	R Fusiform Gyrus	20	−7.045	27	−86	−8
	R Cuneus	34	−6.814	6	−88	29

Note: Contrast: left = left-handers; right = right-handers. Region label according to the Anatomy Toolbox atlas (Eickhoff et al., 2005); R = right; L = left. Extent in voxels, *t* values, and MNI coordinates (*x, y, z*) in Talairach space for each region are displayed.

TABLE 4.4 Between-group result for motor execution (ME) right hand

ME right hand

Contrast	Region label	Extent	t value	MNI coordinates x	y	z
left>right-handers	R Superior Occipital Gyrus	224	11.003	20	−91	11
	R Superior Temporal Gyrus	69	8.426	67	−35	13
	R Fusiform Gyrus	88	7.660	47	−66	−16
	R Lingual Gyrus	88	6.238	44	−86	−12
	L Calcarine Gyrus	146	7.468	−14	−106	−5
	L Lingual Gyrus	146	6.145	−32	−97	−10
	R Cerebellum (VI)	84	7.444	31	−55	−23
	L Heschl's Gyrus	51	7.190	−37	−28	19
	L Cerebellum (III)	34	6.867	−14	−35	−19
	L Middle Orbital Gyrus	100	6.828	−23	62	−7
	R Cerebellum (Crus 2)	47	6.721	47	−57	−39
	R Cerebellum (VI)	19	6.712	22	−79	−16
	R Inferior Temporal Gyrus	34	6.602	51	−3	−28
right>left-handers	L Cerebellum (VI)	122	−7.556	−8	−71	−10
	R Cuneus	42	−7.369	4	−82	33
	L Calcarine Gyrus	98	−7.367	4	−84	17
	L Posterior-Medial Frontal	25	−6.730	−3	−5	74

Note: Contrast: left = left-handers; right = right-handers. Region label according to the Anatomy Toolbox atlas (Eickhoff et al., 2005); R = right; L = left. Extent in voxels, *t* values, and MNI coordinates (*x*, *y*, *z*) in Talairach space for each region are displayed.

TABLE 4.5 Between-group result for motor imagery (MI) both hands

MI both hands

Contrast	Region label	Extent	t value	MNI coordinates x	y	z
left>right-handers	R Calcarine Gyrus	58	−8.379	17	−91	8
	L Cerebellum (VI)	23	−7.830	−8	−86	−10
	R Cerebellum (VI)	29	−6.805	20	−80	−16
right>left-handers	R Lingual Gyrus	158	10.159	4	−70	6
	L Lingual Gyrus	63	7.102	−12	−82	4
	L Middle Occipital Gyrus	39	7.030	−41	−91	13
	L Inferior Occipital Gyrus	31	6.296	−52	−77	1
	L Lingual Gyrus	21	6.287	2	−84	6

Note: Contrast: left = left-handers; right = right-handers. Region label according to the Anatomy Toolbox atlas (Eickhoff et al., 2005); R = right; L = left. Extent in voxels, *t* values, and MNI coordinates (*x*, *y*, *z*) in Talairach space for each region are displayed.

TABLE 4.6 Between-group result for motor execution (ME) both hands

ME both hands

Contrast	Region label	Extent	t value	MNI coordinates		
				x	y	z
left>right-handers	R Cerebellum (Crus 1)	365	−9.6644	47.26	−67.808	−15.5
	R Cerebellum (VI)	365	−8.723	29.29	−57.026	−19.1
	R Fusiform Gyrus	365	−6.863	25.696	−76.793	−4.7
	R Cerebellum (VI)	151	−9.4907	20.305	−78.59	−15.5
	R Posterior-Medial Frontal	168	−8.874	7.726	−10.304	72.7
	L Precentral Gyrus	91	−8.4842	−42.59	−12.101	54.7
	L Cerebellum (VI)	89	−8.2542	−8.447	−83.981	−10.1
	R Calcarine Gyrus	86	−8.1945	20.305	−89.372	11.5
	R Precentral Gyrus	19	−7.6947	20.305	−22.883	76.3
	R Superior Temporal Gyrus	26	−7.6334	68.824	−35.462	13.3
	L Superior Parietal Lobule	119	−7.5787	−24.62	−60.62	61.9
	R Middle Occipital Gyrus	90	−7.4959	32.884	−92.966	18.7
	L Rolandic Operculum	56	−7.4297	−35.402	−31.868	24.1
	L Inferior Parietal Lobule	83	−7.3103	−42.59	−46.244	60.1
	L Cerebellum (Crus 1)	18	−6.8733	−42.59	−74.996	−13.7
	R Superior Temporal Gyrus	33	−6.4218	54.448	−31.868	22.3
	R IFG (pars opercularis)	10	−6.3779	41.869	5.869	27.7
	R Posterior-Medial Frontal	26	−6.3252	9.523	−12.101	58.3
	R Postcentral Gyrus	25	−6.2936	43.666	−24.68	52.9
	R Inferior Parietal Lobule	14	−6.201	31.087	−46.244	58.3
	L Superior Temporal Gyrus	7	−6.0591	−65.951	−49.838	22.3
	L Postcentral Gyrus	5	−6.0498	−53.372	−19.289	36.7
	L Cerebellum (III)	6	−6.0418	−10.244	−37.259	−19.1
right>left-handers	R Lingual Gyrus	60	7.8647	4.132	−69.605	7.9
	R Calcarine Gyrus	33	7.3718	13.117	−78.59	20.5
	L Olfactory cortex	21	7.3046	−3.056	20.245	−6.5
	R Precuneus	14	7.0805	20.305	−48.041	11.5
	L Cuneus	26	6.6208	−1.259	−82.184	31.3
	R Cerebellum (VIII)	13	6.5786	32.884	−64.214	−51.5
	L Calcarine Gyrus	8	6.2525	−8.447	−98.357	2.5
	L Posterior-Medial Frontal	5	6.162	−4.853	−3.116	65.5
	L Superior Medial Gyrus	5	5.9946	−10.244	68.764	7.9
	L Insula Lobe	8	5.9795	−38.996	7.666	6.1
	R Putamen	5	5.7883	16.711	5.869	−4.7
	L Cerebellum (III)	7	5.6799	−10.244	−37.259	−10.1

Note: Contrast: left = left-handers; right = right-handers. Region label according to the Anatomy Toolbox atlas (Eickhoff et al., 2005); R = right; L = left. Extent in voxels, *t* values, and MNI coordinates (*x*, *y*, *z*) in Talairach space for each region are displayed.

TABLES 5 **Within-group results**

TABLE 5.1 Within-group result of motor imagery (MI) for left-handers

Left-handed group MI						
				MNI coordinates		
Contrast	Region label	Extent	*t* value	*x*	*y*	*z*
left >right hand	L Lingual Gyrus	254	10.254	−12	−80	6
	R Lingual Gyrus	214	8.625	10	−89	1
	L Cerebellum (VI)	149	8.277	−12	−71	−7
right >left hand	R Calcarine Gyrus	201	−12.429	15	−79	11
	L Calcarine Gyrus	118	−8.480	−10	−95	1
	R Lingual Gyrus	53	−6.788	10	−68	−5

Note: Contrast: left = left-handers; right = right-handers. Region label according to the Anatomy Toolbox atlas (Eickhoff et al.; 2005); R = right; L = left. Extent in voxels, *t* values, and MNI coordinates (*x, y, z*) in Talairach space for each region are displayed.

TABLE 5.2 Within-group result of motor imagery (MI) for right-handers

Right-handed group MI						
				MNI coordinates		
Contrast	Region label	Extent	*t* value	*x*	*y*	*z*
left >right hand	L Lingual Gyrus	178	10.986	−8	−79	6
	R Lingual Gyrus	83	7.194	6	−89	1
right >left hand	R Lingual Gyrus	259	−11.787	13	−75	8
	L Lingual Gyrus	42	−6.050	−10	−89	−5

Note: Contrast: left = left-handers; right = right-handers. Region label according to the Anatomy Toolbox atlas (Eickhoff et al., 2005); R = right; L = left. Extent in voxels, *t* values, and MNI coordinates (*x, y, z*) in Talairach space for each region are displayed.

TABLE 5.3 Within-group result of motor execution (ME) for left-handers

Left-handed group ME						
				MNI coordinates		
Contrast	Region label	Extent	t value	x	y	z
left >right hand	R Postcentral Gyrus	6,721	32.979	40	−25	53
	R Precentral Gyrus	6,721	17.578	24	−25	76
	R MCC	6,721	13.937	6	−16	51
	L Cerebellum (IV-V)	4,300	21.683	−23	−48	−25
	L Cerebellum (VIII)	4,300	15.571	−19	−59	−53
	R Rolandic Operculum	1,732	12.672	44	−17	20
	R Thalamus	1,732	10.520	19	−21	4
	R Lingual Gyrus	145	8.436	10	−88	1
	R Insula Lobe	19	6.084	38	4	13
right >left hand	L Postcentral Gyrus	4,934	−18.400	−43	−21	53
	L Postcentral Gyrus	4,934	−29.170	−46	−23	58
	L Postcentral Gyrus	4,934	−11.534	−28	−39	60
	L Paracentral Lobule	4,934	−7.968	−14	−30	80
	R Cerebellum (IX)	2,855	−16.188	13	−62	−48
	Cerebellar Vermis (4/5)	2,855	−10.687	6	−66	−5
	R Calcarine Gyrus	305	−14.206	15	−77	10
	L Rolandic Operculum	1,014	−13.324	−43	−21	19
	L Putamen	1,014	−11.967	−32	−12	1
	L MCC	672	−13.104	−5	−19	49
	L Thalamus	237	−12.068	−17	−21	4
	L Calcarine Gyrus	266	−8.912	−10	−95	2
	L Amygdala	21	−7.430	−21	−10	−8
	R Superior Frontal Gyrus	6,721	8.569	22	−17	73

Note: Contrast: left = left-handers; right = right-handers. Region label according to the Anatomy Toolbox atlas (Eickhoff et al., 2005); R = right; L = left. Extent in voxels, *t* values, and MNI coordinates (*x, y, z*) in Talairach space for each region are displayed.

TABLE 5.4 Within-group result of motor execution (ME) for right-handers

Right-handed group ME						
				MNI coordinates		
Contrast	Region label	Extent	*t* value	*x*	*y*	*z*
left >right hand	R Postcentral Gyrus	5,720	34.931	40	−26	55
	R Precentral Gyrus	5,720	10.346	22	−23	74
	R Posterior-Medial Frontal	5,720	7.914	10	−3	74
	L Cerebellum (VIII)	7,258	16.667	−19	−59	−53
	L Cerebellum (IV-V)	7,258	16.543	−5	−62	−14
	R Rolandic Operculum	1,709	13.167	44	−19	19
	R Thalamus	1,709	10.556	15	−17	6
	R Amygdala	1,709	9.945	27	−1	−12
	L Lingual Gyrus	256	11.984	−10	−79	6
	R MCC	720	11.623	6	−17	51
	R Lingual Gyrus	132	7.174	8	−89	2
right >left hand	L Precentral Gyrus	6,444	−5.490	−14	−19	76
	L Postcentral Gyrus	6,444	−7.731	−26	−34	64
	L Postcentral Gyrus	6,444	−32.030	−44	−25	60
	L Postcentral Gyrus	6,444	−14.928	−23	−41	64
	L Paracentral Lobule	6,444	−9.795	−12	−23	80
	Location not in atlas	7,258	−22.063	17	−52	−21
	R Cerebellum (VIII)	7,258	−17.324	17	−61	−52
	R Lingual Gyrus	7,258	−11.488	13	−75	6
	L Rolandic Operculum	2,212	−17.128	−44	−21	19
	L Putamen	2,212	−14.842	−32	−12	1
	L MCC	1,202	−15.512	−5	−10	51
	L Calcarine Gyrus	138	−7.541	−10	−95	2

Note: Contrast: left = left-handers; right = right-handers. Region label according to the Anatomy Toolbox atlas (Eickhoff et al., 2005); R = right; L = left. Extent in voxels, *t* values, and MNI coordinates (*x*, *y*, *z*) in Talairach space for each region are displayed.

TABLES 6 **Between-task results (ME vs. MI)**

TABLE 6.1   Between-task result for left-handers' left hand

Left-handers—left hand				MNI coordinates		
Contrast	Region label	Extent	t value	x	y	z
ME>MI	R Postcentral Gyrus	3,829	28.288	40	−26	53
	R Precentral Gyrus	3,829	13.866	31	−26	73
	L Cerebellum (IV-V)	1,839	12.407	−5	−64	−14
	Cerebellar Vermis (4/5)	1,839	6.680	−1	−48	1
	R Rolandic Operculum	1,775	15.037	44	−19	19
	R Insula Lobe	1,775	8.080	40	2	13
	R Postcentral Gyrus	1,775	5.672	65	−12	24
	L Cerebellum (VIII)	676	13.313	−21	−57	−55
	R MCC	709	9.649	6	−17	51
	R Thalamus	201	8.831	19	−21	4
	L Rolandic Operculum	150	8.427	−50	−26	19
	L Postcentral Gyrus	285	8.316	−55	−21	38
	R Amygdala	129	7.920	27	0	−10
	L Superior Orbital Gyrus	19	7.386	−14	33	−17
MI>ME	L Posterior-Medial Frontal	232	−9.633	1	9	55
	L Precentral Gyrus	97	−8.577	−34	−5	51
	L Paracentral Lobule	20	−6.091	−7	−34	60

Note: Contrast: ME, motor execution; MI, motor imagery. Region label according to the Anatomy Toolbox atlas (Eickhoff et al., 2005); R = right; L = left. Extent in voxels, *t* values, and MNI coordinates (*x, y, z*) in Talairach space for each region are displayed.

TABLE 6.2   Between-task result for left-handers' right hand

Left-handers—right hand				MNI coordinates		
Contrast	Region label	Extent	t value	x	y	z
ME>MI	L Postcentral Gyrus	3,868	26.881	−46	−23	58
	L Postcentral Gyrus	3,868	6.937	−23	−44	58
	R Cerebellum (VIII)	616	14.757	17	−62	−50
	L Rolandic Operculum	1,234	14.674	−46	−26	20
	L Putamen	1,234	8.570	−32	−12	1
	L MCC	476	10.522	−5	−19	49
	R Postcentral Gyrus	134	7.855	60	−16	44
	R Rolandic Operculum	89	6.556	51	−21	19
	R Superior Temporal Gyrus	21	6.404	62	−14	13
MI>ME	L Posterior-Medial Frontal	309	−9.460	1	8	55
	L Precentral Gyrus	81	−8.615	−37	−7	51
	L Superior Parietal Lobule	19	−6.208	−17	−64	55
	R Superior Orbital Gyrus	20	−5.979	19	17	−8

Note: Contrast: ME, motor execution; MI, motor imagery. Region label according to the Anatomy Toolbox atlas (Eickhoff et al., 2005); R = right; L = left. Extent in voxels, *t* values, and MNI coordinates (*x, y, z*) in Talairach space for each region are displayed.

TABLE 6.3 Between-task result for right-handers' left hand

Right-handers—left hand

Contrast	Region label	Extent	t value	MNI coordinates x	y	z
ME>MI	R Postcentral Gyrus	4,052	−30.377	40	−26	55
	L Cerebellum (IV-V)	2,338	−18.726	−17	−52	−23
	R Rolandic Operculum	1,249	−16.379	51	−21	19
	L Cerebellum (VIII)	591	−13.470	−19	−59	−53
	L Olfactory cortex	70	−9.030	−5	22	4
	R Thalamus	163	−8.814	15	−17	6
	R Posterior-Medial Frontal	358	−8.813	4	−7	51
	R Rolandic Operculum	84	−8.497	42	−1	17
	Cerebellar Vermis (3)	220	−8.151	2	−43	2
	L Superior Temporal Gyrus	160	−8.105	−57	−23	15
	L Postcentral Gyrus	266	−7.980	−55	−21	38
	L Insula Lobe	38	−6.739	−46	−3	8
	R Thalamus	20	−6.625	4	−17	11
MI>ME	L Posterior-Medial Frontal	196	8.880	−10	6	56
	L Paracentral Lobule	457	8.385	−14	−28	71
	R Precentral Gyrus	76	8.238	40	0	51
	R Cerebellum (IX)	33	8.069	11	−59	−37
	L Postcentral Gyrus	63	7.752	−44	−12	38
	Cerebellar Vermis (3)	29	7.477	2	−48	−17
	R Posterior-Medial Frontal	164	7.475	11	−23	67
	R Middle Temporal Gyrus	34	6.850	44	−64	11
	L Precentral Gyrus	33	6.727	−37	−3	49
	L Middle Occipital Gyrus	49	6.726	−52	−80	4
	R Caudate Nucleus	22	6.595	20	−21	29
	R Superior Parietal Lobule	27	6.452	26	−59	62
	L Superior Parietal Lobule	20	6.424	−26	−59	64
	R Middle Temporal Gyrus	36	6.404	62	−32	2
	L Middle Frontal Gyrus	28	6.209	−23	−7	53

Note: Contrast: ME, motor execution; MI, motor imagery. Region label according to the Anatomy Toolbox atlas (Eickhoff et al., 2005); R = right; L = left. Extent in voxels, *t* values, and MNI coordinates (*x, y, z*) in Talairach space for each region are displayed.

TABLE 6.4 Between-task result for right-handers' right hand

Right-handers—right hand						
				MNI coordinates		
Contrast	Region label	Extent	t value	x	y	z
ME>MI	L Postcentral Gyrus	4,369	28.377	−44	−25	60
	L Rolandic Operculum	1,885	17.155	−48	−25	19
	L Insula Lobe	1,885	9.708	−46	−3	8
	Cerebellar Vermis (6)	1,686	8.356	1	−79	−8
	R Cerebellum (IX)	521	13.064	13	−64	−48
	L MCC	512	12.431	−7	−9	49
	L Posterior-Medial Frontal	27	8.019	−5	−14	76
	R Rolandic Operculum	99	7.668	63	−17	19
	R Lingual Gyrus	19	6.839	24	−75	4
	R Insula Lobe	45	6.791	40	−14	10
	L Cerebellum (Crus 1)	23	6.408	−12	−89	−21
MI>ME	R Cerebellum (VIII)	819	−6.124	11	−75	−35
	L Posterior-Medial Frontal	279	−9.799	−8	4	55
	R Precentral Gyrus	54	−8.053	19	−28	69
	L Precentral Gyrus	255	−8.049	−39	−5	53
	L Middle Temporal Gyrus	174	−7.945	−53	−75	13
	L Postcentral Gyrus	149	−7.923	−43	−12	37
	R Middle Frontal Gyrus	19	−7.574	38	0	49
	L Middle Temporal Gyrus	209	−7.116	−55	−53	20
	L Cerebellum (VIII)	37	−7.073	−8	−71	−35
	L Middle Frontal Gyrus	128	−7.040	−48	31	35
	L Precentral Gyrus	41	−6.842	−48	2	46
	L Superior Frontal Gyrus	171	−6.718	−25	56	6
	L Paracentral Lobule	31	−6.637	−5	−32	65
	L ACC	74	−6.600	−8	27	28
	L Middle Orbital Gyrus	29	−6.580	−35	45	2
	L Cerebellum (Crus 1)	76	−6.511	−30	−66	−35
	L Cerebellum (Crus 2)	83	−6.510	−41	−61	−37
	R Middle Temporal Gyrus	29	−6.468	63	−37	8
	R Middle Temporal Gyrus	61	−6.402	54	−70	10
	R Caudate Nucleus	23	−6.356	10	17	1
	L Inferior Parietal Lobule	81	−6.353	−39	−52	55
	L IFG (pars triangularis)	30	−6.275	−30	26	8
	L IFG (pars orbitalis)	19	−6.103	−34	24	−5
	L Cerebellum (VIII)	19	−6.035	−19	−73	−39
	L Middle Frontal Gyrus	22	−5.954	−41	36	26

Note: Contrast: ME, motor execution; MI, motor imagery. Region label according to the Anatomy Toolbox atlas (Eickhoff et al., 2005); R = right; L = left. Extent in voxels, *t* values, and MNI coordinates (*x, y, z*) in Talairach space for each region are displayed.